Development of Novel Dihydrofuro[3,4-*d*]pyrimidine Derivatives as HIV-1 NNRTIs to Overcome the Highly Resistant Mutant Strains F227L/V106A and K103N/Y181C

Dongwei Kang, [†,*] Yanying Sun,[†] Da Feng, [†] Shenghua Gao,[†] Zhao Wang, [†] Lanlan Jing, [†] Tao Zhang,[†] Xiangyi Jiang,[†] Hao Lin,[†] Erik De Clercq, [§] Christophe Pannecouque, [§] Peng Zhan,[†,&,*] and Xinyong Liu[†, &,*]

[†] *Department of Medicinal Chemistry, Key Laboratory of Chemical Biology (Ministry of Education), School of Pharmaceutical Sciences, Cheeloo College of Medicine, Shandong University, 44 West Culture Road, 250012 Jinan, Shandong, PR China*

[§] *Rega Institute for Medical Research, Laboratory of Virology and Chemotherapy, K.U. Leuven, Herestraat 49 Postbus 1043 (09.A097), B-3000 Leuven, Belgium.*

[&] *China-Belgium Collaborative Research Center for Innovative Antiviral Drugs of Shandong Province, 44 West Culture Road, 250012 Jinan, Shandong, PR China*

ABSTRACT

Here, we reported the design, synthesis, structure−activity relationship studies, antiviral activity, enzyme inhibition, and druggability evaluation of dihydrofuro[3,4-*d*]pyrimidine derivatives as a potent class of HIV-1 NNRTIs. Compounds **14b** (EC_{50} = 5.79-28.3 nM) and **16c** (EC_{50} = 2.85-18.0 nM) exhibited superior potency against a panel of HIV-1 resistant strains. Especially for the changeling mutations F227L/V106A and K103N/Y181C, both compounds exhibited remarkably improved activity compared to those of ETR and RPV. Moreover, **14b** and **16c** showed modest RT enzyme inhibitory (IC_{50} = 0.14-0.15 μM), which demonstrated that they acted as HIV-1 NNRTIs. Furthermore, **14b** and **16c** exhibited favorable pharmacokinetic and safety properties, making them as excellent leads for further

development.

INTRODUCTION

Acquired immunodeficiency syndrome (AIDS), which is caused by human immunodeficiency virus (HIV), remains a serious epidemic disease since it was first reported in 1981[1]. In the life cycle of HIV-1, reverse transcriptase (RT) is a key enzyme that responsible for reverse transcription of viral single-stranded RNA into double-stranded DNA, and inhibition of the HIV-1 RT leads to viral load suppression declines in patients[2]. Non-nucleoside reverse transcriptase inhibitors (NNRTIs) bind to an allosteric pocket of HIV-1 RT and their mechanism of action is noncompetitively inhibit DNA polymerization, have the advantage of efficient potency, higher selectivity and favorable pharmacokinetics[3, 4]. There have six NNRTIs drugs have been approved with HIV-1 RT as drug target[5], including the first-generation drug delavirdine (DLV) nevirapine (NVP) and efavirenz (EFV), and the second-generation drug etravirine (ETR), rilpivirine (RPV) and doravirine (DOR). The first-generation NNRTIs exhibited favorable activity against HIV-1 wild-type (WT) strain, while the single mutants K103N and Y181C seriously limited their clinic application[6, 7]. Although the second-generation NNRTIs exhibited promising activity against WT HIV-1 and these single mutant (K103N, Y181C), the newly emerging double mutant strains (F227L/V106A and K103N/Y181C) seriously reducing their effectiveness[8, 9]. As shown in **Figure 1**, ETR (EC_{50} = 45.4 nM) exhibited weaker efficacy toward K103N/Y181C[10] and RPV (EC_{50} = 81.6 nM) exhibited sharply decreased potency toward F227L/V106A[9] compared with their potency to WT HIV-1.

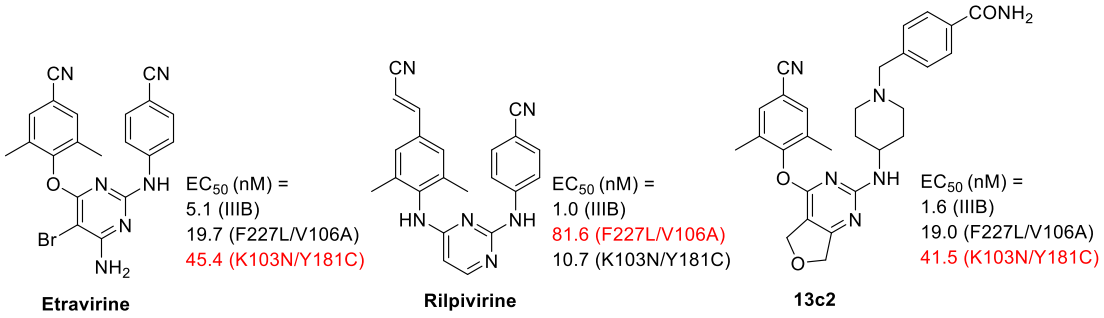

Figure 1. Structures and activities of etravirine, rilpivirine and our previously reported lead compound **13c2**.

With the aim to discover potent HIV-1 NNRTIs with enhanced activity against resistance-associated variants, extensive structural modification has been conducted using ETR and RPV as leads[11-17]. For example, the dihydrofuro[3,4-*d*]pyrimidine derivative **13c2** was demonstrated with higher resistance profiles and lower cytotoxicity (CC_{50} > 250 μM)[10]. Although **13c2** displayed better activity against F227L/V106A (EC_{50} = 19.0 nM), its potency toward K103N/Y181C (EC_{50} = 41.5 nM) much weaker than that toward WT HIV-1 (EC_{50} = 1.6 nM). To achieve the goal of overcoming the resistance to mutant HIV-1 strains K103N/Y181C and F227L/V106A strains simultaneously, detailed structural modifications of **13c2** were performed in this work. We kept the privileged dihydrofuro[3,4-*d*]pyrimidine structure unchanged, and the cyano group of **13c2** was replaced with cyano vinyl to establish more effective π-π interactions with the amino acids in hydrophobic pocket, including Tyr181, Tyr188, and Trp229. Then the piperidine-substituted benzyl motif of the right wing was replaced by nine different structural motifs with a classical scaffold hopping strategy (**Figure 2**). Most of these newly introduced motifs contain hydrogen bond donor and receptors, with the hope to develop more stronger hydrogen bonding interactions with the RT pocket, including the amino acid residues Lys101, Lys103

and Lys 104. A total of 25 novel anti-HIV-1 compounds were obtained to get a more distinct understanding of the structure-activity relationships (SARs) of the NNRTIs binding pocket (NNIBP) tolerant region I and discover potent inhibitors with promising antiviral activities.

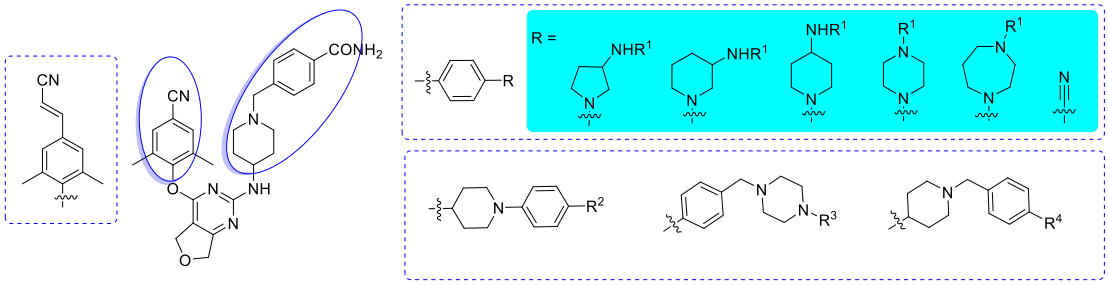

Figure 2. Design strategy of the target compounds

CHEMISTRY

RESULTS AND DISCUSSION

All the novel anti-HIV-1 compounds were screened for their biological activity to WT HIV-1 (IIIB) and mutant strain K103N/Y181C in MT-4 cells with MTT method[18]. The selected potent inhibitors were tested for their activity against other common NNRTIs-resistant strains, including L100I, K103N, Y181C, Y188L, E138K, and F227L/V106A. ETR, RPV and DOR were acted as positive controls. The values of EC_{50} (anti-HIV-1 potency, concentration of compound required to acquire 50% protection of cell cultures against HIV-1-induced cytopathicity), CC_{50} (cytotoxicity, concentration required to reduce the viability of mock-infected cell cultures by 50%), and SI (selectivity index, CC_{50}/EC_{50} ratio) of these novel inhibitors were determined and shown in **Tables 1-4**.

Table 1. Anti-HIV-1 (IIIB and K103N/Y181C) Activity, Cytotoxicity and SI value of **8a-j** and **12**

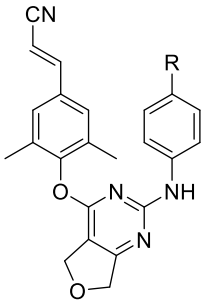

Compds	R	EC_{50} (nM)		CC_{50} (μM)	SI	
		IIIB	K103N/Y181C		IIIB	RES056
8a	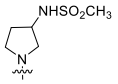	9.95 ± 2.72	38265 ± 452	109 ± 34.9	10961	29
8b	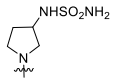	159 ± 65.4	48249 ± 2430	41.6 ± 9.60	260	< 1
8c	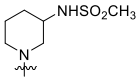	128 ± 75.4	> 13900	13.9 ± 3.82	109	< 1
8d	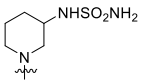	128 ± 72.5	> 24200	24.2 ± 1.51	188	< 1
8e	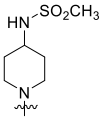	79.9 ± 55.5	> 17500	17.5 ± 4.30	219	< 1
8f	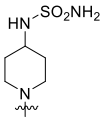	530 ± 268	> 14500	14.5 ± 9.09	27	< 1
8g	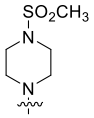	11.0 ± 3.38	> 183000	183 ± 21.0	16629	< 1
8h	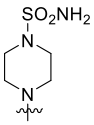	62.6 ± 15.7	> 168000	168 ± 10.2	2692	< 1
8i	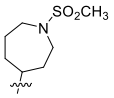	26.2 ± 5.55	> 109000	109 ± 19.1	4153	< 1
8j	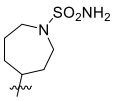	90.9 ± 41.5	> 7480	7.48 ± 5.82	82	< 1
12	CN	2.20 ± 0.35	64.2 ± 4.57	36.6 ± 15.7	16636	570
ETR	-	3.93 ± 0.73	72.3 ± 25.1	> 4.59	> 1168	> 64
RPV	-	1.00 ± 0.27	10.7 ± 7.96	3.98	3989	371
DOR[a]	-	13.3 ± 3.75	14.5 ± 5.87	>293	>21805	>20096

[a] Results from ref **19**.

Table 1 showed the activity of target compounds **8a-j** and **12**. Compound **12** (R = CN) exhibited the most effective activity to HIV-1 IIIB (EC_{50} = 2.20 nM) and K103N/Y181C (EC_{50} = 64.2 nM), being comparable to that of ETR (EC_{50} = 3.93 nM and 72.3 nM, respectively). Although **12** displayed inferior activity against K103N/Y181C than those of RPV (EC_{50} = 10.7 nM) and DOR (EC_{50} = 14.5 nM)[19], it was demonstrated with much lower cytotoxicity (CC_{50} = 36.6 μM) and higher SI values (SI = 16636 and 570) than that of RPV (CC_{50} = 3.98 μM, SI = 3989 and 371). Elaboration with pyrrole, pyridine, piperazine and azepane group at the R position result in a decrease in the activity of the compounds against HIV-1 IIIB (**8a-j,** EC_{50} = 9.95-159 nM). However, most compounds (**8c-j**) lost their activity for the mutant strain RES056. Comparison of their activity concluded the preliminary SARs that SO_2CH_3 group was more favorable for increasing activity against HIV-1 IIIB than that of SO_2NH_2 group (**8a** *vs* **8b**, **8e** *vs* **8f**, **8g** *vs* **8h**, and **8i** *vs* **8j**).

Based on the preliminary activity screening results, the most potent inhibitor **12** was further evaluated for its potency against NNRTIs-resistant strains. As shown in **Table 4**, **12** proved to be a highly potent inhibitor of HIV-1 mutant strains L100I, K103N, Y181C, Y188L and E138K (EC_{50} = 2.38-33.2 nM), being equivalent to that of ETR (EC_{50} = 4.65-48.7 nM). However, **12** (EC_{50} = 62.6 nM) exhibited decreased potency than that of ETR (EC_{50} = 21.4 nM) toward double mutant strains F227L+V106A.

Replacement of the benzene-heterocycle motif of **8a-j** with piperidine-benzene motif yielded target compounds **13a-c** and **14a-c**, and their activity was depicted in

Table 2. Most derivatives (**13a-c** and **14b**) displayed superior potency (EC_{50} = 2.38 – 6.30 nM) against HIV-1 IIIB strain, being superior to than that of DOR (EC_{50} = 13.3 nM) and comparable to that of ETR (EC_{50} = 3.93 nM) and RPV (EC_{50} = 1.00 nM). Moreover, all derivatives exhibited much decreased cytotoxicity than that of RPV. In the case of K103N/Y181C, the activities of compounds **13a-c** (EC_{50} = 992-1298 nM) dramatically decreased compared to ETR and RPV. **14b** was proved to be the most active inhibitor (EC_{50} = 27.9 nM), being comparable to that of RPV. Moreover, the activity of **14c** was equivalent to that of ETR, providing an EC_{50} value of 88.9 nM. Then, we tested the drug resistance profiles of the most promising compounds **14b** and **14c**. As depicted in **Table 4**, **14b** was potent inhibitor of the tested mutant HIV-1 strains (EC_{50} = 5.79 - 28.3 nM). Especially for the double mutant strain F227L+V106A, **14b** (EC_{50} = 5.79 nM) was demonstrated with significantly improved potency, affording 3.6 and 14-fold enhancement relative to the reference ETR (EC_{50} = 21.4 nM) and RPV (EC_{50} = 81.6 nM). Moreover, **14b** also exhibited much increased activity against Y188L than those of ETR (EC_{50} = 48.7 nM) and RPV (EC_{50} = 79.4 nM), with EC_{50} value of 28.3 nM. All results indicated that **14b** showed effective resistance profiles. However, replacement of the $NHSO_2CH_3$ group of **14b** with $NHSO_2NH_2$ (**14c**, EC_{50} = 13.1-1248 nM) led to much decreased potency.

Table 2. Anti-HIV-1 (IIIB and K103N/Y181C) Activity, Cytotoxicity and SI value of **13a-c** and **14a-c**

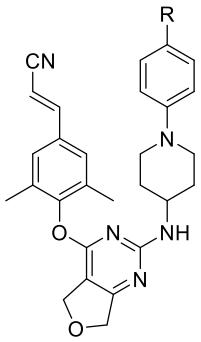

Compds	R	EC_{50} (nM)		CC_{50} (μM)	SI	
		IIIB	K103N/Y181C		IIIB	RES056
13a	SO_2NH_2	4.18 ± 0.96	1298 ± 268	27.3 ± 1.19	6531	23
13b	SO_2CH_3	6.30 ± 1.85	1198 ± 178	104 ± 76.9	16507	87
13c	$CONH_2$	2.38 ± 0.56	992 ± 671	> 233	> 97899	> 234
14a	NH_2	35.4 ± 6.28	249 ± 49.9	9.14 ± 1.69	258	37
14b	$NHSO_2CH_3$	6.17 ± 1.68	27.9 ± 1.05	38.8 ± 5.32	6293	1391
14c	$NHSO_2NH_2$	16.8 ± 13.4	88.9 ± 15.3	23.0 ± 1.45	1370	260
ETR	-	3.93 ± 0.73	72.3 ± 25.1	> 4.59	> 1168	> 64
RPV	-	1.00 ± 0.27	10.7 ± 7.96	3.98	3989	371
DOR	-	13.3 ± 3.75	14.5 ± 5.87	>293	>21805	>20096

To further explore more adaptive group of the tolerant region I of the RT-binding pocket and discover more potent HIV-1 inhibitors, the privileged piperidine-methane-benzene and benzene-methane-piperazine scaffolds reported in our previous research was introduced to the right wing. As shown in **Table 3**, compounds **16a-e** featuring piperidine-methane-benzene motif on the right wing yielded excellent activity to HIV-1 IIIB (EC_{50} = 2.85-8.32 nM) and RES056 (EC_{50} = 11.7-65.0 nM), respectively. **16c** yielded the most effective potency, providing an EC_{50} values of 2.85 and 11.7 nM, which was superior to that of ETR and comparable

to that of RPV and DOR. Moreover, **16c** was demonstrated with reduced cytotoxicity (CC_{50} = 36.6 μM) and higher SI values (SI = 8450 and 2061) than those of RPV (CC_{50} = 3.98 μM, SI = 3989 and 371). Although compounds **18a-b** featuring benzene-methane-piperazine motif displayed promising activity to HIV-1 IIIB, their potency against RES056 was sharply decreased (**18a**, EC_{50} > 8020 nM; **18b**, EC_{50} = 1165 nM).

Table 3. Anti-HIV-1 (IIIB and K103N/Y181C) Activity, Cytotoxicity and SI value of **16a-f** and **18a-b**

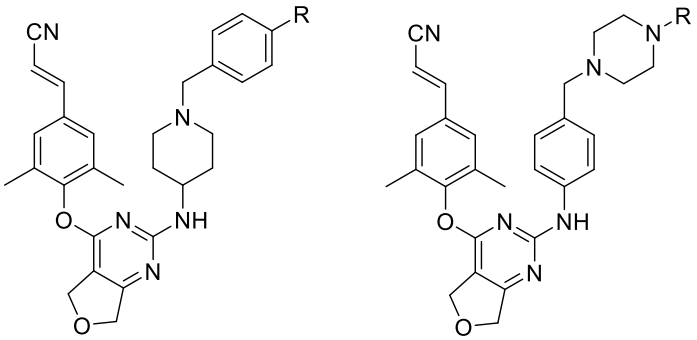

Compds	R	EC_{50} (nM)		CC_{50} (μM)	SI	
		IIIB	K103N/Y181C		IIIB	RES056
16a	SO_2NH_2	6.24 ± 1.80	24.7 ± 5.25	14.7 ± 3.51	2361	595
16b	SO_2CH_3	4.33 ± 0.17	34.6 ± 1.77	9.79 ± 0.68	2260	283
16c	$CONH_2$	2.85 ± 1.17	11.7 ± 4.22	24.1 ± 0.59	8450	2061
16d	NO_2	8.32 ± 2.58	65.0 ± 19.4	6.67 ± 2.59	801	103
16e	NH_2	3.37 ± 0.93	53.5 ± 28.6	27.0 ± 0.94	8020	505
16f	CF_3	19.5 ± 5.54	190 ± 15.6	5.01 ± 0.94	256	26
18a	SO_2NH_2	20.3 ± 8.95	> 8020	8.02 ± 1.93	395	<1
18b	SO_2CH_3	6.55 ± 1.71	1165 ± 250	> 44.5	>6803	>38
ETR	-	3.93 ± 0.73	72.3 ± 25.1	> 4.59	>1168	>64
RPV	-	1.00 ± 0.27	10.7 ± 7.96	3.98	3989	371

DOR	-	13.3 ± 3.75	14.5 ± 5.87	>293	>21805	>20096

Furthermore, compounds **16a-f** and **18b** were further tested for their potency against the whole viral panel. As shown in **Table 4**, **16c** was demonstrated with exceptionally potent antiviral activity, with EC_{50} values of 3.90 nM (L100I), 2.14 nM (K103N), 6.09 nM (Y181C), 18.0 nM (Y188L), 6.76 nM (E138K) and 9.67 nM (F227L+V106A), respectively. Especially for Y188L and F227L+V106A, the activity of **16c** was about 4.4- and 8.4-fold higher than that of RPV. Moreover, compounds **16a** and **16b** inhibited L100I, Y181C and F227L+V106A more potently than those of ETR. **18b** also showed promising antiviral activity against K103N and E138K, with EC_{50} values of 8.29 nM and 8.38 nM, being equipotent to that of ETR; however, it exhibited decreased potency (EC_{50} = 7901 nM) against Y188L. These results contribute to the SAR that the right wing of the compound is critical for activity, especially for mutant HIV-1 strains, and piperidine-methane-benzene motif was proved to be the best choice for the right wing.

Table 4. Activity against Mutant HIV-1 Strains of Selected Compounds

Compds	**EC_{50} (nM)**					
	L100I	**K103N**	**Y181C**	**Y188L**	**E138K**	**F227L+V106A**
12	3.18 ± 1.11	2.38 ± 0.23	10.9 ± 0.92	33.2 ± 3.10	7.39 ± 1.77	62.6 ± 13.4
14b	12.4 ± 2.02	6.91 ± 1.28	8.91 ± 1.78	28.3 ± 6.25	7.66 ± 0.35	5.79 ± 1.46
14c	1248 ± 128	13.1 ± 2.85	46.5 ± 1.78	141 ± 68.7	34.6 ± 6.07	19.9 ± 6.65
16a	5.12 ± 1.91	5.97 ± 0.73	7.71 ± 2.04	38.0 ± 4.85	10.3 ± 1.00	11.9 ± 2.89
16b	5.18 ± 0.78	6.47 ± 0.73	9.96 ± 3.63	41.4 ± 3.03	15.4 ± 5.13	16.3 ± 8.86
16c	3.90 ± 1.03	2.14 ± 0.36	6.09 ± 1.23	18.0 ± 9.76	6.76 ± 2.49	9.67 ± 1.67
16d	10.4 ± 1.31	7.78 ± 0.49	26.8 ± 7.81	94.0 ± 33.5	21.7 ± 5.53	60.5 ± 6.00

16e	10.2 ± 4.80	5.58 ± 1.17	9.36 ± 0.81	51.4 ± 6.71	9.16 ± 1.14	37.6 ± 9.48
16f	34.5 ± 7.20	30.1 ± 7.11	65.6 ± 16.9	282 ± 119	129 ± 36.4	199 ± 35.8
18b	30.4 ± 16.4	8.29 ± 0.90	58.1 ± 11.5	7901 ± 170	8.38 ± 0.87	112 ± 24.0
ETR	17.4 ± 4.28	4.65 ± 0.64	20.2 ± 2.68	48.7 ± 21.8	15.4 ± 3.40	21.4 ± 7.12
RPV	1.54 ± 0.00	1.31 ± 0.36	4.73 ± 0.48	79.4 ± 0.77	5.75 ± 0.11	81.6 ± 21.2

To confirm the target of these inhibitors, they were evaluated for their inhibitory activity to WT HIV-1 RT using the ELISA method (Roche assay kit)[20]. The result was shown in IC_{50} values (concentration of compounds required for 50% inhibition). As depicted in **Table 5**, the highly active inhibitors **8a**, **8g**, **8i**, **12**, **13a-c**, **14a-c**, **16a-e**, and **18b** also displayed strong enzyme inhibition activity with IC_{50} values of 0.06-0.23 μM, which were superior or comparable to that of NVP (IC_{50} = 0.31 μM). The weaker inhibitors to HIV-1 IIIB showed reduced inhibitory activity, such as **8b**, **8c** and **8f** (IC_{50} = 1.06 μM, 1.24 μM and 1.32 μM, respectively). The results demonstrated that there is a certain correlation between enzyme activity and cytoactive. However, their RT inhibitory activity less potent than their activity in HIV cell culture compared to that of ETR. These differences could be attributed the template-specific variations of polymerase progression and HIV-RT-RNA binding affinity[11]. Anyhow, the current result could validate that their binding target is HIV-1 RT.

Table 5. HIV-1 RT Inhibitory Activity of Compounds

Compds	**IC_{50} (μM)**	**Compds**	**IC_{50} (μM)**
8a	0.18 ± 0.03	**14a**	0.18 ± 0.01
8b	1.06 ± 0.16	**14b**	0.15 ± 0.08
8c	1.24 ± 0.04	**14c**	0.12 ± 0.02
8d	0.78 ± 0.07	**16a**	0.14 ± 0.01

8e	0.46 ± 0.17	**16b**	0.15 ± 0.06
8f	1.32 ± 0.16	**16c**	0.14 ± 0.04
8g	0.18 ± 0.03	**16d**	0.18 ± 0.01
8h	0.71 ± 0.03	**16e**	0.19 ± 0.00
8i	0.23 ± 0.06	**16f**	0.36 ± 0.02
8j	0.09 ± 0.002	**18a**	0.28 ± 0.00
12	0.06 ± 0.005	**18b**	0.15 ± 0.03
13a	0.06 ± 0.005	**NVP**	0.31 ± 0.08
13b	0.07 ± 0.006	**ETR**[a]	0.01 ± 0.00
13c	0.06 ± 0.001		

[a] Results from reference[10].

Molecular Docking Studies.

To further learn the binding pattern of these novel obtained NNRTIs with NNIBP, the most potent compounds **14b** and **16c** were selected to perform the molecular docking studies using SurflexeDock SYBYLX 2.0. The co-crystal structures of F227L/V106A HIV-1 RT/**25a** (PDB: 6duf) and K103N/Y181C HIV-1 RT/**25a** (PDB: 6c0r) were served as the input structures[21]. The docking results were visualized by PyMOL.

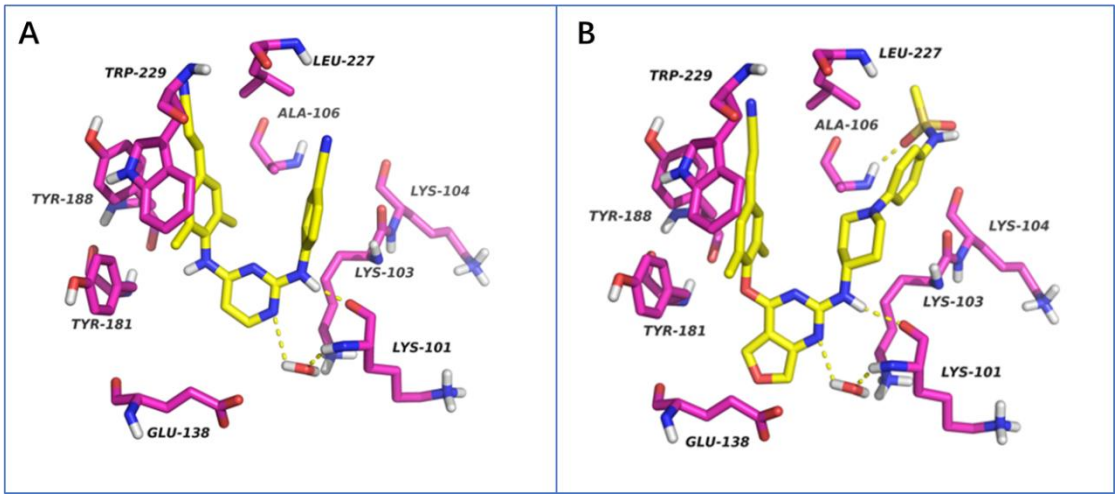

Figure 3. Binding modes of RPV (**A**) and **14b** (**B**) with HIV-1 F227L/V106A RT (PDB: 6duf).

The conformation of **14b** and **16c** weren't affected by the slightly changes of NNIBP caused by the F227L/V106A double mutation (**Figure 3**). Both compounds still adopt an U shape in the binding pocket, but the Phe227 to Leu227 substitution in RT greatly reduce the binding interface between these compounds and NNIBP, and led to the hydrophobic interactions decreased of the Phe227 side chain with the dimethylphenyl ring of both compounds. The dramatic changes of π-π interactions result in a decreased activity of RPV (**Figure 3A**). In the case of compound **14b** (**Figure 3B**), the decreased binding affinity caused by the mutation could be alleviated by the newly developed hydrogen-bonding of the sulfonamide group and backbone nitrogen of the mutated Ala106. Moreover, the *NH* linker in the right wing acts as a hydrogen bond donor and retained the hydrogen bond with the carbonyl of Lys101, the *N* atom of the dihydrofuro[3,4-*d*]pyrimidine scaffold acts as a hydrogen bond receptor developed water-mediated hydrogen bonds with amino of Lys101. All these interactions explained the effective potency of **14b** toward F227L/V106A mutant strain.

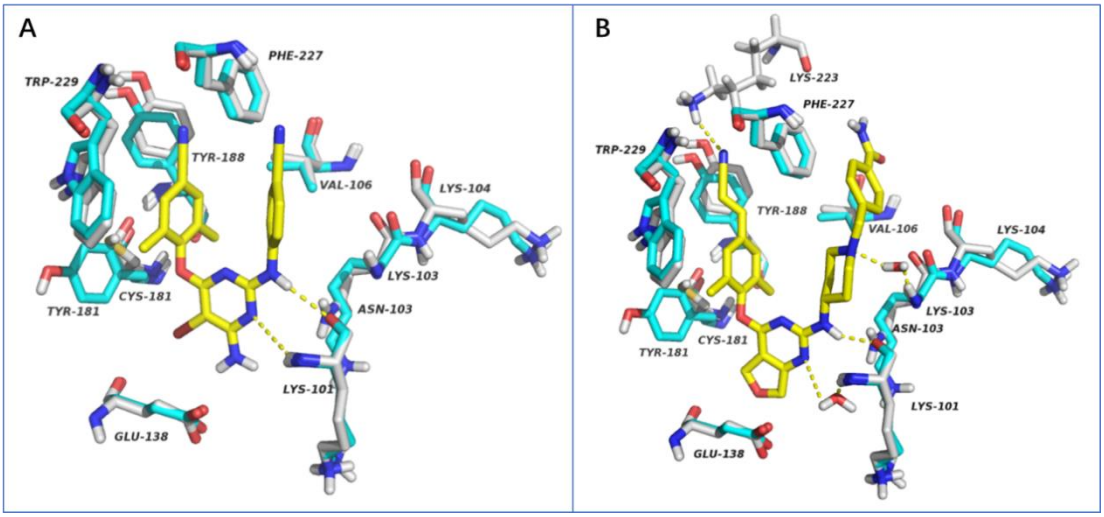

Figure 4. Superimposed of binding modes of WT RT/ETR on to K103N/Y181C RT/ETR (**A**) and WT RT/**16c** on to K103N/Y181C RT/**16c** (**B**) (PDB: 6c0r). The amino acid residues of WT RT are colored in cyan and K103N/Y181C RT are colored in gray.

As for the more disruptive double mutation K103N/Y181C, the reference drug ETR and **16c** were selected to perform the molecular docking. Although the hydrogen bond interactions are retained in ETR and Lys101 (**Figure 4A**), the Tyr181 to Cys181 substitution abolishes the favorable hydrophobic interactions between ETR and NNIBP, which was responsible for the greatly reduced activity of ETR against K103N/Y181C. In the regard to compound **16c**, the sharply weakened π-π interactions between **16c** and Cys181 are compensated by the abundant of hydrogen-bonding force, including the cyano vinyl group with Lys223, the central scaffold and *NH* linker with the backbone of Lys101, and the piperidine with Asn103 (**Figure 4B**). All these hydrogen-bonding interactions account for the potent activity of **16c** against K103N/Y181C.

***In Vivo* Pharmacokinetics Study**

Considering the improved drug-resistance profiles and the confirmed target,

compounds **14b** and **16c** were further evaluated for their *in vivo* pharmacokinetic profiles in Sprague Dawley rats PK models. The PK parameters are provided in **Table 6** and **Figure 5**. Compound **14b** showed moderate clearance (CL = 36.7 mL/min/kg) after a single *iv* dose (2 mg/kg) in rat PK studies, the maximum concentration (C_{max}) was 756 ng/mL and displayed a terminal half-life time of 1.11 h. Moreover, the terminal half-life time could reach 1.47 h after being oral administration, and the oral bioavailability (*F*) was 16.6%. Compared to **14b**, **16c** was demonstrated with a slightly improved clearance (CL = 66.3 mL/min/kg) and reduced half-life time ($T_{1/2}$ = 0.88 h) after *iv* injection. In oral administration, the plasma concentration reached maximum at 2.12 h with C_{max} of 250 ng/mL. Notably, **16c** was demonstrated with improved bioavailability (*F* = 32.1%), which could be explained by its greater solubility compared to that of **14b** (**Table 7**).

Table 6. Pharmacokinetic Profile of **14b** and **16c**[a]

Subject	$T_{1/2}$ (h)	T_{max} (h)	C_{max} (ng/mL)	AUC_{0-t} (h*ng/mL)	$AUC_{0-\infty}$ (h*ng/mL)	CL (mL/min/kg)	F (%)
14b (iv)[b]	1.11 ± 0.05	0.033	756 ± 16.0	903 ± 16.1	908 ± 14.7	36.7 ± 0.58	-
14b (po)[c]	1.47 ± 0.24	1.00 ± 0.00	307 ± 23.0	727 ± 39.5	753 ± 51.1	-	16.6
16c (iv)[b]	0.88 ± 0.07	0.033	480 ± 14.5	490 ± 7.21	503 ± 11.0	66.3 ± 1.46	-
16c (po)[c]	1.05 ± 0.05	2.12 ± 0.03	250 ± 22.4	801 ± 51.2	809 ± 61.4	-	32.1

[a] PK parameter (mean ± SD, n = 3), [b] The intravenous dose is 2 mg/kg, [c] The oral dose is 10 mg/kg.

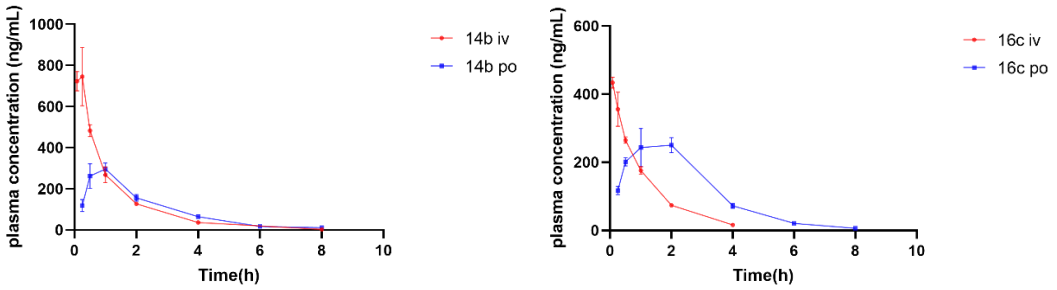

Figure 5. The plasma concentration-time curve of **14b** and **16c** in rats.

Table 7. The Aqueous Solubility of **14b** and **16c**

Compds	Aqueous solubility (μg/mL)[a]		
	pH 7.4	pH 7.0	pH 2.0
14b	2.10	10.1	124
16c	5.24	25.4	187
ETR	<1	<1	127
RPV	<1	<1	103

[a] Measured with HPLC method.

Safety Assessment

The acute toxicity experiment of compounds **14b** and **16c** was performed in healthy Kunming mice. 30 Kunming mice were grouped into three, and two groups were given **14b** and **16c** with dosage of 2000 mg/kg by oral administration, and one group was selected as Ctr group. The experimental mice did not show any abnormal symptoms during the following 7 days. Moreover, the weight of mice did not change significantly compared with the control group (**Figure 6**). All the results indicated that compounds **14b** and **16c** have no acute toxicity in Kunming mice with a dosage of 2000 mg/kg.

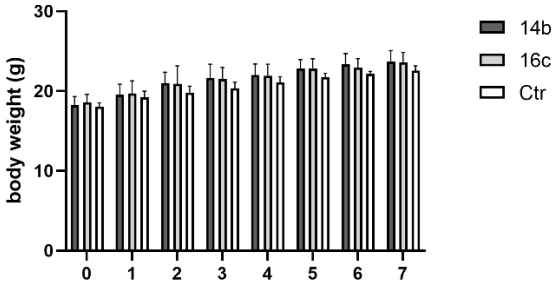

Figure 6. Body weight changes of Kunming mice in three groups.

Conclusion

Here, we reported our intellectual work to discover effective HIV-1 NNRTIs by modifying the tolerant region I of the RT-binding pocket, and totally twenty-five new anti-HIV-1 compounds were designed and obtained. The results demonstrated that compounds **14b** (EC_{50} = 5.79-28.3 nM) and **16c** (EC_{50} = 2.85-18.0 nM) exhibited exceptionally potent activity to HIV-1 IIIB and NNRTIs-resistant strains. Especially for the changeling double strains F227L/V106A and K103N/Y181C, both compounds exhibited remarkably improved activity compared to those of ETR and RPV. Moreover, the HIV-1 RT enzyme inhibitory assay indicated that the target of these novel compounds was RT. The molecular docking studies have been performed to show the binding mode of **14b** and **16c**, explaining why they are resilient to the highly resistant strains F227L/V106A and K103N/Y181C. Moreover, **14b** and **16c** exhibited favorable pharmacokinetic profiles in SD rats (F = 16.6% and 32.1%, $T_{1/2}$ = 1.47 h and 1.05 h, respectively) and safety in Kunming mice (LD_{50} > 2000 mg/kg). The effective and favorable profiles *in vitro* and *in vivo* makes them as excellent leads for further development.

EXPERIMENTAL SECTION

Chemistry

All reactions were carried out in reagent-grade or better solvents. Evaporation of the solvents was performed with a rotary evaporator (IKA, RV-10) under reduced pressure. ^{1}H-NMR and ^{13}C-NMR spectra were recorded in DMSO-d_6 on a Bruker AV-400 spectrometer. NMR chemical shift (δ) are quoted in ppm referenced to the DMSO-d_6 peak set at 2.49 ppm. The reaction was monitored by thin layer chromatography (TLC), and spots were visualized by irradiation with UV light. The purity of target compounds >95%, which was determined by analytical HPLC (Shimadzu SPD-20A/20AV).

Scheme **1** shows the synthesis of the intermediates **3a-e** for target compounds **8a-j** in **Table 1**. The starting material 4-fluoronitrobenzene (**1**) was treated with 3-*N*-Boc-aminopyrrolidine, 3-Boc-aminopiperidine, 4-Boc-aminopiperidine, 1-Boc-piperazine, and 1-Boc-hexahydro-1,4-diazepine obtained intermediates **2a-e** respectively, which provided **3a-e** *via* reduction reaction under the condition of Pd/C and H_2. As shown in Scheme **2**, the nucleophilic substitution of starting compound **4** with 3,5-dimethyl-4-hydroxybenzaldehyde obtained intermediate **5**, which was treated with $(EtO)_2P(O)CH_2CN$ yielding intermediate **6** *via* Wittig−Horner reaction[12]. Then Buchwald−Hartwig reaction of **6** and the obtained intermediates **3a** under the condition that BINAP and $Pd_2(dba)_3$, followed by deprotection of Boc group furnished the free amine **7**. Treatment **7** with methanesulfonyl chloride or sulfamoyl chloride afforded the target compounds **8a-b** *via* acylation reaction. In an analogous way, target compounds **8b-j** were prepared, only with the difference that intermediate

6 was reacted with **3b-e** (Scheme **S1**).

Scheme 1. Synthesis of Intermediates 3a-e[a]

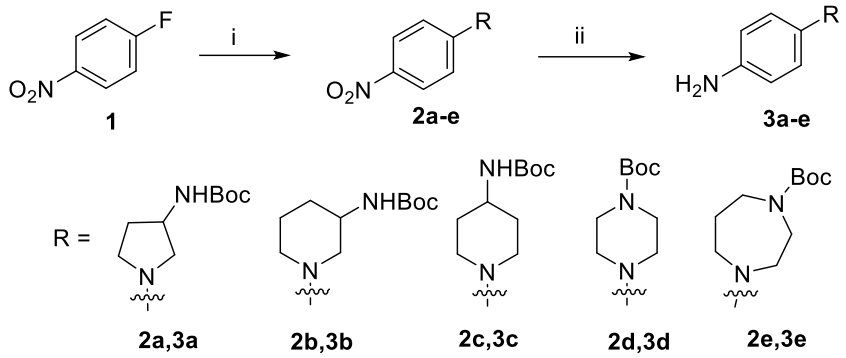

[a] **Reagents and conditions:** (i) DMSO, 100℃; (ii) MeOH, Pd/C, H_2, r.t.

Scheme 2. Synthesis of Target Compounds 8a-b[a]

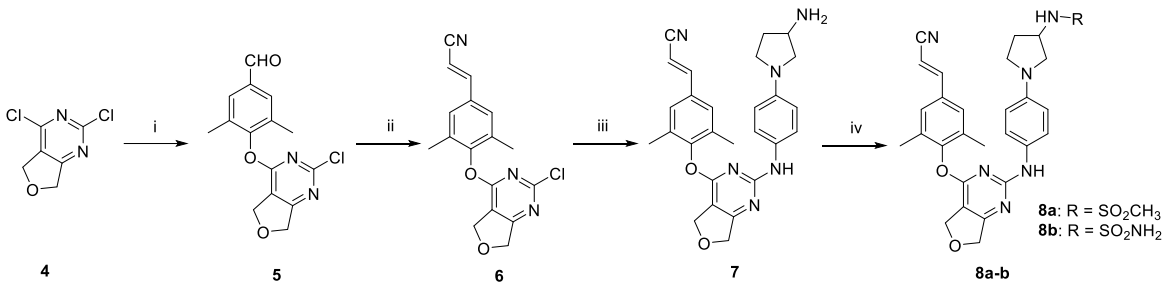

[a] **Reagents and conditions:** (i) DMF, 3,5-dimethyl-4-hydroxybenzaldehyde, K_2CO_3, r.t.; (ii) THF, *t*-BuOK, $(EtO)_2P(O)CH_2CN$, 0°C to r.t.; (iii) 1,4-dioxane, **3a-e**, $Pd_2(dba)_3$, BINAP, Cs_2CO_3, 90°C, N_2; then DCM, TFA, r.t.; (iv) DCM, CH_3SO_2Cl or NH_2SO_2Cl, Et_3N, r.t.

Schemes 3-4 shows the synthesis of compounds in **Table 2**. Different substituted fluorobenzenes **9a-c** were reacted with *tert*-butyl piperidin-4-ylcarbamate to obtain intermediates **10a-c**. The Boc group of **10a-c** and **2c** were removed to give intermediates **11a-d**, which were subsequently coupled with intermediate **6** affording compounds **13a-d** *via* Buchwald−Hartwig reaction. Then the nitro group of **13d** was reduced to the amino group **14a**, followed by treating with methanesulfonyl chloride

or sulfamoyl chloride gave the target compounds **14b-c**.

Scheme 3. Synthesis of Intermediates 11a-d[a]

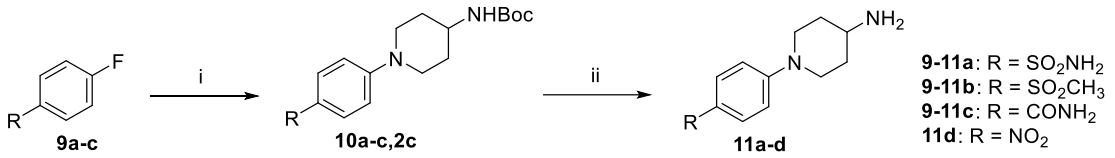

[a] **Reagents and conditions:** (i) DMSO, *tert*-butyl piperidin-4-ylcarbamate, 120℃; (ii) DCM, TFA, r.t.

Scheme 4. Synthesis of Target Compounds 12, 13a-d, and 14a-c[a]

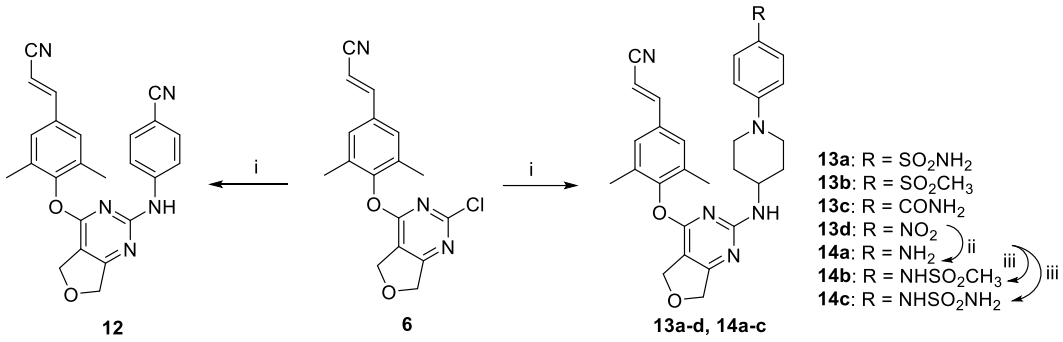

[a] **Reagents and conditions:** (i) 1,4-dioxane, **11a-d** or 4-aminobenzonitrile, $Pd_2(dba)_3$, BINAP, Cs_2CO_3, 90°C, N_2; (ii) MeOH, Pd/C, H_2, r.t.; (iii) DCM, CH_3SO_2Cl or NH_3SO_2Cl, Et_3N, r.t.

Schemes 5 shows the synthesis of target compounds **16a-f** and **18a-b**. Nucleophilic substitution of **6** with *tert*-butyl 4-aminopiperidine-1-carboxylate, followed by deprotection of Boc group furnished **15**. Then nucleophilic substitution of **15** with substituted benzyl chloride (or bromine) afforded target compounds **16a-f**. Buchwald−Hartwig reaction of **6** with the previous prepared intermediate *tert*-butyl 4-(4-aminobenzyl)piperazine-1-carboxylate[22] in the presence of BINAP and $Pd_2(dba)_3$, followed by cleavage of the Boc group, obtained intermediate **17**. Finally, **17** was converted to target compounds **18a-b** *via* acylation reaction.

Scheme 5. Synthesis of Target Compounds 16a-f[a]

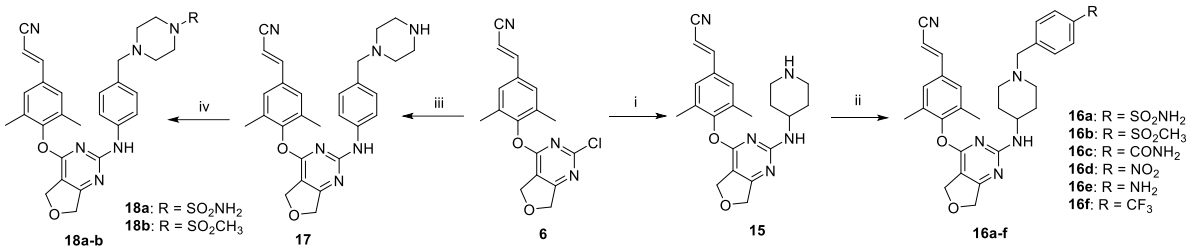

[a] **Reagents and conditions:** (i) DMF, *tert*-butyl 4-aminopiperidine-1-carboxylate, K_2CO_3, 120°C; then DCM, TFA, r.t.; (ii) DMF, substituted benzyl chloride (bromine), K_2CO_3, r.t.; (iii) 1,4-dioxane, *tert*-butyl 4-(4-aminobenzyl)piperazine-1-carboxylate, BINAP, $Pd_2(dba)_3$, Cs_2CO_3, 90°C, N_2; then DCM, TFA, r.t.; (iv) DCM, CH_3SO_2Cl or NH_2SO_2Cl, Et_3N, r.t.

General Synthesis Procedure for 3a-e

The starting materials 4-fluoronitrobenzene (**1**, 2.82 g, 20 mmol) and 3-*N*-Boc-aminopyrrolidine (3.72 g, 20 mmol) were added in DMSO (30 mL), and the reaction was conducted at 100˚C for 6 h. Then water (150 mL) was added after the solution was cooled to room temperature. The obtained precipitate was collected by filtered and dried to get crude **2a**, which was added to 30 mL methanol for next step. 10% palladium on carbon (0.42 g, 0.20 mmol) was added and stirred for 12 h in hydrogen. The solution was filtered and evaporated to yield intermediate **3a** as white solid, which was used in the following step without purification. In addition, 3-Boc-aminopiperidine, 4-Boc-aminopiperidine, 1-Boc-piperazine, and 1-Boc-hexahydro-1,4-diazepine were used as the reactive materials to reacted with 1 yielded **3b-e**, respectively.

4-((2-chloro-5,7-dihydrofuro[3,4-*d*]pyrimidin-4-yl)oxy)-3,5-dimethylbenzaldehyde

(**5**)

The starting material 2,4-dichloro-5,7-dihydrofuro[3,4-*d*]pyrimidine (**4**, 3.78 g, 20 mmol), 4-hydroxy-3,5-dimethylbenzaldehyde (3.00 g, 20 mmol), and K_2CO_3 (3.40 g, 24 mmol) were added in DMF (50 mL) and stirred at rt for 5 h. Then the obtained white solid was filtered and recrystallized in DMF/H_2O to get white solid **5** in 92% yield, mp: 241-243°C. ^{1}H NMR (400 MHz, DMSO-d_6) δ 9.83 (s, 1H, CHO), 7.44 (s, 2H, C_3,C_5-Ph-H), 4.92 (s, 2H, O-CH_2), 4.76 (s, 2H, O-CH_2), 2.06 (s, 6H). ESI-MS: m/z 305.2 $[M + 1]^+$ $C_{15}H_{13}ClN_2O_3$ (304.06).

(*E*)-3-(4-((2-chloro-5,7-dihydrofuro[3,4-*d*]pyrimidin-4-yl)oxy)-3,5-dimethylphenyl)acrylonitrile (**6**)

A solution of $(EtO)_2P(O)CH_2CN$ (0.70 g, 3.93 mmol) and t-BuOK (0.74 g, 6.56 mmol) in THF (10 mL) was reacted 1 h at 0°C, and then compound **5** (1.0 g, 3.28 mmol) in THF (10 mL) was dripped into the mixture within 1 h. When the reaction completed (monitored by TLC), water (100 mL) was added and the precipitate was filtered to afford **6** as a white solid in 74% yield, mp: 256-258°C. ^{1}H NMR (400 MHz, DMSO-d_6) δ 7.69 (d, J = 16.7 Hz, 1H, ArCH＝), 7.44 (s, 2H, C_3,C_5-Ph-H), 6.50 (d, J = 16.4 Hz, 1H, ＝CHCN), 4.92 (s, 2H, O-CH_2), 4.76 (s, 2H, O-CH_2), 2.06 (s, 6H). ESI-MS: m/z 328.3 $[M + 1]^+$, 350.4 $[M + Na]^+$. $C_{17}H_{14}ClN_3O_2$ (327.08).

General Synthesis Procedure for 7 and S1-4 (supporting information)

To a solution of compound **6** (0.66 g, 2.0 mmol) and **3a-e** (2.4 mol) were dissolved in dioxane (20 mL) added $Pd_2(dba)_3$ (0.02 g, 0.02 mmol), BINAP (0.012 g, 0.02 mmol), and Cs_2CO_3 (1.96 g, 6.0 mmol). The reaction was performed in a nitrogen atmosphere. The reaction was stirred at 120°C for 6-12 h (monitored by

TLC), and then the solvent was removed in vacuo. Dissolved the residue in DCM and extracted with saturated sodium chloride. Then the organic phase was evaporated and used for next step. Then TFA (1.48 mL, 20 mmol) was added to the solution, and the mixture was stirred for 6 h. The mixture was alkalized to alkaline (pH = 9), and the organic layer was washed with water. The crude product was purified and recrystallized from EA/PE afforded compounds **7** and **S1-4**.

(*E*)-3-(4-((2-((4-(3-aminopyrrolidin-1-yl)phenyl)amino)-5,7-dihydrofuro[3,4-*d*]pyrimidin-4-yl)oxy)-3,5-dimethylphenyl)acrylonitrile (**7**)

Yield 39%, white solid, mp 136-138°C. ^{1}H NMR (400 MHz, DMSO-d_6) δ 9.28 (s, 1H, NH), 7.69 (d, J = 16.4 Hz, 1H, ArCH═), 7.51-7.48 (m, 2H), 7.44 (s, 2H, C_3,C_5-Ph-H), 7.21 (d, J = 6.8 Hz, 2H), 6.51 (d, J = 16.7 Hz, 1H, ═CHCN), 4.92 (s, 2H, O-CH_2), 4.78 (s, 2H, O-CH_2), 4.02-3.83 (m, 2H), 3.14-3.07 (m, 2H), 2.21-2.19 (m, 1H), 2.11 (s, 6H), 1.90-1.41 (m, 4H). ESI-MS: m/z 547.3 $[M + 1]^+$, 569.5 $[M + Na]^+$. $C_{27}H_{28}N_6O_2$ (468.23).

General Synthesis Procedure for 8a-j

Intermediates **7** (or **S1-S4**, 2.0 mmol) and Et_3N (0.34 mL, 2.4 mmol) were added to anhydrous DCM (15 mL), followed by addition of the methylsulfonyl chloride or sulfamoyl chloride (2.4 mmol) at 0°C. After stirred at rt for 8 h, to the mixture was added saturated sodium chloride and extracted with DCM. Dried the DCM phase with anhydrous Na_2SO_4, purified and recrystallized from EA/PE got compounds **8a-j**.

(*E*)-*N*-(1-(4-((4-(4-(2-cyanovinyl)-2,6-dimethylphenoxy)-5,7-dihydrofuro[3,4-*d*]pyrimidin-2-yl)amino)phenyl)pyrrolidin-3-yl)methanesulfonamide (**8a**)

Yield 69%, white solid, mp 169-171°C. ^{1}H NMR (400 MHz, DMSO-d_6) δ 9.31 (s, 1H, NH), 7.70 (s, 1H), 7.48-7.22 (m, 4H), 7.08 (s, 1H), 6.71 (d, J = 15.7 Hz, 1H, ＝CHCN), 6.18-6.09 (m, 2H), 5.01 (s, 2H, O-CH_2), 4.81 (s, 2H, O-CH_2), 4.09-3.86 (m, 2H), 3.17-3.08 (m, 2H), 2.97 (s, 3H, SO_2CH_3), 2.21-2.18 (m, 1H), 2.11 (s, 6H), 1.90-1.88 (m, 2H). ^{13}C NMR (100 MHz, DMSO-d_6) δ 173.6, 164.7, 163.0, 137.5, 133.2, 131.4, 131.1, 129.9, 128.1, 124.0, 111.6, 72.2, 69.5, 54.0, 52.6, 50.6, 46.2, 40.9, 32.2, 29.0, 16.7. ESI-MS: m/z 547.3 $[M + 1]^+$, 569.5 $[M + Na]^+$. $C_{28}H_{30}N_6O_4S$ (546.20). HPLC purity: 96.52%.

(*E*)-*N*-(1-(4-((4-(4-(2-cyanovinyl)-2,6-dimethylphenoxy)-5,7-dihydrofuro[3,4-*d*]pyrimidin-2-yl)amino)phenyl)pyrrolidin-3-yl)aminosulfonamide (**8b**)

Yield 36%, white solid, mp 196-198°C. ^{1}H NMR (400 MHz, DMSO-d_6) δ 9.32 (s, 1H, NH), 7.70-7.68 (m, 1H), 7.47-7.25 (m, 4H), 7.23-7.02 (m, 3H), 6.71 (d, J = 16.4 Hz, 1H, ＝CHCN), 6.20-6.12 (m, 2H), 5.02 (s, 2H, O-CH_2), 4.84 (s, 2H, O-CH_2), 4.10-3.84 (m, 2H), 3.16 (s, 2H), 2.20 (s, 1H), 2.10 (s, 6H), 1.94-1.89 (m, 2H). ^{13}C NMR (100 MHz, DMSO-d_6) δ 173.8, 164.7, 162.9, 150.7, 146.5, 137.3, 133.2, 131.8, 129.9, 128.4, 124.0, 118.5, 111.6, 103.7, 72.2, 69.5, 52.6, 50.6, 46.2, 32.8, 29.0, 16.7. ESI-MS: m/z 548.2 $[M + 1]^+$, 570.4 $[M + Na]^+$. $C_{27}H_{29}N_7O_4S$ (547.20). HPLC purity: 97.35%.

(*E*)-*N*-(1-(4-((4-(4-(2-cyanovinyl)-2,6-dimethylphenoxy)-5,7-dihydrofuro[3,4-*d*]pyrimidin-2-yl)amino)phenyl)piperidin-3-yl)methanesulfonamide (**8c**)

Yield 60%, white solid, mp 181-183°C. ^{1}H NMR (400 MHz, DMSO-d_6) δ 9.45 (s, 1H, NH), 7.79-7.64 (m, 2H), 7.54 (s, 2H, C_3,C_5-Ph-H), 7.18-7.10 (m, 2H),

6.63-6.45 (m, 3H), 5.05 (s, 2H, O-CH_2), 4.85 (s, 2H, O-CH_2), 3.45 (q, *J* = 7.6 Hz, 2H), 2.94 (s, 3H, SO_2CH_3), 2.63 (t, *J* = 11.9 Hz, 2H), 2.11 (s, 6H), 1.90 (d, *J* = 12.6 Hz, 2H), 1.64-1.44 (m, 3H). ^{13}C NMR (100 MHz, DMSO-d_6) δ 173.8, 162.8, 160.7, 152.4, 150.6, 148.6, 146.0, 132.5, 131.8, 129.6, 128.6, 119.9, 118.3, 116.4, 103.6, 96.7, 95.4, 72.2, 69.4, 50.6, 48.7, 41.6, 32.9, 16.6. ESI-MS: m/z 561.5 $[M + 1]^+$, 583.4 $[M + Na]^+$. $C_{29}H_{32}N_6O_4S$ (560.22). HPLC purity: 97.08%.

(*E*)-*N*-(1-(4-((4-(4-(2-cyanovinyl)-2,6-dimethylphenoxy)-5,7-dihydrofuro[3,4-*d*]pyri midin-2-yl)amino)phenyl)piperidin-3-yl)methanesulfonamide (**8d**)

Yield 29%, white solid, mp 215-117°C. ^{1}H NMR (400 MHz, DMSO-d_6) δ 9.47 (s, 1H, NH), 7.78-7.69 (m, 2H), 7.54 (s, 2H, C_3,C_5-Ph-H), 7.36 (d, *J* = 3.9 Hz, 2H), 7.23-7.02 (m, 2H), 6.79-6.67 (m, 1H), 6.63-6.47 (m, 2H), 5.04 (s, 2H, O-CH_2), 4.85 (s, 2H, O-CH_2), 3.36-3.35 (m, 1H), 3.17 (q, *J* = 12.9 Hz, 2H), 2.11 (s, 6H), 1.96-1.70 (m, 2H), 1.64-1.34 (s, 4H). ^{13}C NMR (100 MHz, DMSO-d_6) δ 173.8, 164.9, 163.0, 162.8, 160.7, 152.3, 150.5, 148.6, 146.3, 137.5, 133.2, 132.9, 131.8, 129.5, 128.6, 123.9, 119.9, 116.9, 115.1, 96.7, 72.2, 69.5, 56.3, 51.7, 47.7, 30.7, 23.1, 16.6. ESI-MS: m/z 562.1 $[M + 1]^+$, 584.3 $[M + Na]^+$. $C_{28}H_{31}N_7O_4S$ (561.22). HPLC purity: 98.32%.

(*E*)-*N*-(1-(4-((4-(4-(2-cyanovinyl)-2,6-dimethylphenoxy)-5,7-dihydrofuro[3,4-*d*]pyri midin-2-yl)amino)phenyl)piperidin-4-yl)methanesulfonamide (**8e**)

Yield 80%, white solid, mp 172-174°C. ^{1}H NMR (400 MHz, DMSO-d_6) δ 9.45 (s, 1H, NH), 7.80-7.63 (m, 2H), 7.54 (s, 2H, C_3,C_5-Ph-H), 7.18-7.12 (m, 2H), 6.65-6.44 (m, 3H), 5.05 (s, 2H, O-CH_2), 4.85 (s, 2H, O-CH_2), 3.53-3.38 (m, 3H), 2.94 (s, 3H, SO_2CH_3), 2.63 (t, *J* = 11.9 Hz, 2H), 2.11 (s, 6H), 1.90 (t, *J* = 12.6 Hz, 2H),

1.67-1.43 (m, 2H). ^{13}C NMR (100 MHz, DMSO-d_6) δ 173.8, 162.8, 160.7, 152.4, 150.6, 148.6, 146.0, 132.5, 131.8, 129.6, 128.6, 119.9, 119.3, 118.3, 116.4, 103.6, 96.7, 95.4, 72.2, 69.4, 50.6, 48.7, 41.6, 32.8, 16.5. ESI-MS: m/z 561.2 $[M + 1]^+$. $C_{29}H_{32}N_6O_4S$ (560.22). HPLC purity: 97.75%.

(*E*)-*N*-(1-(4-((4-(4-(2-cyanovinyl)-2,6-dimethylphenoxy)-5,7-dihydrofuro[3,4-*d*]pyrimidin-2-yl)amino)phenyl)piperidin-4-yl)aminosulfonamide (**8f**)

Yield 24%, white solid, mp 194-196°C. ^{1}H NMR (400 MHz, DMSO-d_6) δ 9.45 (s, 1H, NH), 7.80-7.63 (m, 3H), 7.54 (s, 2H, C_3,C_5-Ph-H), 7.18-7.12 (m, 2H), 6.65-6.44 (m, 3H), 6.40 (d, *J* = 16.7 Hz, 1H, ＝CHCN), 5.07 (s, 2H, O-CH_2), 4.86 (s, 2H, O-CH_2), 3.52-3.41 (m, 3H), 2.63 (t, *J* = 12.2 Hz, 2H), 2.11 (s, 6H), 1.92-1.90 (m, 2H), 1.67-1.51 (m, 2H). ^{13}C NMR (100 MHz, DMSO-d_6) δ 173.8, 162.7, 160.7, 152.4, 150.1, 146.7, 132.5, 132.0, 129.6, 128.6, 119.8, 118.1, 116.4, 104.0, 96.7, 72.7, 69.7, 50.6, 48.7, 32.8, 16.7. ESI-MS: m/z 562.4 $[M + 1]^+$, 584.4 $[M + Na]^+$. $C_{28}H_{31}N_7O_4S$ (561.22). HPLC purity: 98.69%.

(*E*)-3-(3,5-dimethyl-4-((2-((4-(4-(methylsulfonyl)piperazin-1-yl)phenyl)amino)-5,7-dihydrofuro[3,4-*d*]pyrimidin-4-yl)oxy)phenyl)acrylonitrile (**8g**)

Yield 66%, white solid, mp 158-160°C. ^{1}H NMR (400 MHz, DMSO-d_6) δ 9.50 (s, 1H, NH), 7.70 (d, *J* = 16.5 Hz, 1H, ArCH＝), 7.54 (s, 2H, C_3,C_5-Ph-H), 7.13 (s, 2H), 6.60 (s, 2H), 6.52 (d, *J* = 16.7 Hz, 1H, ＝CHCN), 5.05 (s, 2H, O-CH_2), 4.86 (s, 2H, O-CH_2), 3.24 (t, *J* = 5.1 Hz, 4H), 3.07 (t, *J* = 5.0 Hz, 4H), 2.92 (s, 3H, SO_2CH_3), 2.09 (s, 6H). ^{13}C NMR (100 MHz, DMSO-d_6) δ 173.9, 162.8, 160.7, 152.3, 150.6, 145.6, 133.4, 131.8, 129.6, 128.6, 119.9, 119.3, 116.7, 103.8, 96.7, 72.2, 69.5, 49.2,

45.8, 36.2, 34.3, 29.0, 16.5. ESI-MS: m/z 547.1 $[M + 1]^+$, 569.2 $[M + Na]^+$. $C_{28}H_{30}N_6O_4S$ (546.20). HPLC purity: 99.05%.

(*E*)-4-(4-((4-(4-(2-cyanovinyl)-2,6-dimethylphenoxy)-5,7-dihydrofuro[3,4-*d*]pyrimidin-2-yl)amino)phenyl)piperazine-1-sulfonamide (**8h**)

Yield 44%, white solid, mp 185-187°C. ^{1}H NMR (400 MHz, DMSO-d_6) δ 9.51 (s, 1H, NH), 7.70 (d, J = 16.7 Hz, 1H, ArCH═), 7.54 (s, 2H, C_3,C_5-Ph-H), 7.18-7.12 (m, 4H), 6.62-6.58 (m, 2H), 6.52 (d, J = 16.7 Hz, 1H, ═CHCN), 5.08 (s, 2H, O-CH_2), 4.89 (s, 2H, O-CH_2), 3.27-3.24 (m, 4H), 3.07 (t, J = 5.1 Hz, 4H), 2.10 (s, 6H). ^{13}C NMR (100 MHz, DMSO-d_6) δ 173.7, 162.8, 160.6, 152.3, 150.6, 145.7, 133.4, 132.0, 130.1, 128.6, 119.7, 116.7, 103.1, 96.7, 72.5, 69.7, 49.2, 34.3, 29.1, 16.5. ESI-MS: m/z 548.3 $[M + 1]^+$. $C_{27}H_{29}N_7O_4S$ (547.20). HPLC purity: 98.26%.

(*E*)-3-(3,5-dimethyl-4-((2-((4-(4-(methylsulfonyl)-1,4-diazepan-1-yl)phenyl)amino)-5,7-dihydrofuro[3,4-*d*]pyrimidin-4-yl)oxy)phenyl)acrylonitrile (**8i**)

Yield 83%, white solid, mp 164-166°C. ^{1}H NMR (400 MHz, DMSO-d_6) δ 9.35 (s, 1H, NH), 7.70 (d, J = 16.7.0 Hz, 1H, ArCH═), 7.54 (s, 2H, C_3,C_5-Ph-H), 7.23-6.86 (m, 2H), 6.51 (d, J = 16.6 Hz, 1H, ═CHCN), 6.36 (s, 2H), 5.04 (s, 2H, O-CH_2), 4.84 (s, 2H, O-CH_2), 3.59-3.43 (m, 4H), 3.24-3.00 (m, 2H), 2.77 (s, 3H, SO_2CH_3), 2.16-2.12 (m, 2H), 2.11 (s, 6H), 1.91-1.73 (m, 2H). ^{13}C NMR (100 MHz, DMSO-d_6) δ 173.8, 162.8, 160.7, 152.4, 150.6, 148.6, 142.6, 131.8, 130.0, 129.6, 128.6, 120.7, 119.3, 118.4, 111.6, 96.6, 95.4, 72.2, 69.5, 50.4, 47.8, 37.3, 27.6, 16.6. ESI-MS: m/z 561.3 $[M + 1]^+$, 583.5 $[M + Na]^+$. $C_{29}H_{32}N_6O_4S$ (560.22). HPLC purity: 99.35%.

(*E*)-4-(4-((4-(4-(2-cyanovinyl)-2,6-dimethylphenoxy)-5,7-dihydrofuro[3,4-*d*]pyrimidin-2-yl)amino)phenyl)-1,4-diazepane-1-sulfonamide (**8j**)

Yield 33%, white solid, mp 183-185°C. ^{1}H NMR (400 MHz, DMSO-d_6) δ 9.36 (s, 1H, NH), 7.72-7.64 (m, 1H, ArCH═), 7.54 (s, 2H, C_3,C_5-Ph-H), 7.36 (d, J = 7.5 Hz, 2H), 7.23-6.85 (m, 2H), 6.52 (d, J = 16.6 Hz, 1H, ═CHCN), 6.34 (s, 2H), 5.04 (s, 2H, O-CH_2), 4.84 (s, 2H, O-CH_2), 3.49-3.41 (m, 4H), 3.12 – 2.78 (m, 2H), 2.09 (s, 6H), 2.00-1.81 (m, 2H), 1.54-1.33 (m, 2H). ^{13}C NMR (100 MHz, DMSO-d_6) δ 173.8, 162.8, 150.6, 137.5, 131.8, 131.5, 130.1, 129.6, 128.6, 123.9, 119.3, 111.7, 96.6, 72.7, 69.5, 60.7, 50.6, 48.5, 47.4, 46.8, 29.0, 26.8, 16.5. ESI-MS: m/z 562.3 $[M + 1]^+$. $C_{28}H_{31}N_7O_4S$ (561.22). HPLC purity: 96.59%.

General Synthesis Procedure for Compounds 12 and 13a-d

Compound **6** (0.66 g, 2.0 mmol) and 4-aminobenzonitrile (or **11a-d**, 2.4 mol) were dissolved in dioxane (20 mL), and then to the mixture was added $Pd_2(dba)_3$ (0.02 g, 0.02 mmol), BINAP (0.012 g, 0.02 mmol), and Cs_2CO_3 (1.96 g, 6.0 mmol). The reaction was performed at 120°C for 4-10 h (monitored by TLC) in a nitrogen atmosphere. The solution was filtered and added water, and then extracted with EA. Then the EA phase was purified and recrystallized from EA/PE got compounds **12** and **13a-d.**

(*E*)-4-((4-(4-(2-cyanovinyl)-2,6-dimethylphenoxy)-5,7-dihydrofuro[3,4-*d*]pyrimidin-2-yl)amino)benzonitrile (**12**)

Yield 56%, white solid, mp 231-233°C. ^{1}H NMR (400 MHz, DMSO-d_6) δ 9.62 (s, 1H, NH), 7.69 (d, J = 16.7 Hz, 1H, ArCH═), 7.54 (s, 2H, C_3,C_5-Ph-H), 7.52 (d, J

= 8.0 Hz, 2H, C_3,C_5-Ph'-H), 7.19 (d, *J* = 7.8 Hz, 2H, C_2,C_6-Ph'-H), 6.50 (d, *J* = 16.4 Hz, 1H, ＝CHCN), 5.04 (s, 2H, O-CH_2), 4.86 (s, 2H, O-CH_2), 2.10 (s, 6H). ^{13}C NMR (100 MHz, DMSO-d_6) δ 173.9, 163.1, 160.3, 152.2, 150.4, 143.5, 133.0, 131.8, 130.6, 129.7, 128.6, 119.0, 118.6, 104.5, 96.4, 72.2, 69.7, 16.5. ESI-MS: m/z 410.2 $[M + 1]^+$, 432.4 $[M + Na]^+$. $C_{24}H_{19}N_5O_2$ (409.15). HPLC purity: 99.25%.

(*E*)-4-(4-((4-(4-(2-cyanovinyl)-2,6-dimethylphenoxy)-5,7-dihydrofuro[3,4-*d*]pyrimidin-2-yl)amino)piperidin-1-yl)benzenesulfonamide (**13a**)

Yield 44%, white solid, mp 189-190°C. ^{1}H NMR (400 MHz, DMSO-d_6) δ 7.60 (d, *J* = 16.4 Hz, 1H, ArCH＝), 7.54 (s, 2H, C_3,C_5-Ph-H), 7.37-7.27 (m, 2H),7.24 (d, *J* = 7.9 Hz, 2H, C_3,C_5-Ph'-H), 6.92 (d, *J* = 7.9 Hz, 2H, C_2,C_6-Ph'-H), 6.50 (d, *J* = 16.7 Hz, 1H, ＝CHCN), 5.91 (s, 1H, NH), 5.06 (s, 2H, O-CH_2), 4.86 (s, 2H, O-CH_2), 3.64-3.62 (m, 1H), 2.85-2.70 (m, 2H), 2.08 (s, 6H), 1.94-1.21 (m, 6H). ^{13}C NMR (100 MHz, DMSO-d_6) δ 163.0, 162.7, 150.9, 148.5, 143.0, 139.7, 131.8, 129.4, 128.7, 128.5, 126.9, 119.3, 118.7, 115.7, 104.6, 69.5, 62.0, 52.3, 31.8, 16.5. ESI-MS: m/z 547.1 $[M + 1]^+$. $C_{28}H_{30}N_6O_4S$ (546.20). HPLC purity: 98.33%.

(*E*)-3-(3,5-dimethyl-4-((2-((1-(4-(methylsulfonyl)phenyl)piperidin-4-yl)amino)-5,7-dihydrofuro[3,4-*d*]pyrimidin-4-yl)oxy)phenyl)acrylonitrile (**13b**)

Yield 62%, white solid, mp 176-178°C. ^{1}H NMR (400 MHz, DMSO-d_6) δ 7.90-7.82 (m, 2H), 7.60-7.58 (m, 1H, ArCH＝), 7.56 (d, *J* = 8.0 Hz, 2H), 7.44 (s, 2H, C_3,C_5-Ph-H), 6.42 (d, *J* = 16.4 Hz, 1H, ＝CHCN), 5.92 (s, 1H, NH), 4.92 (s, 2H, O-CH_2), 4.78 (s, 2H, O-CH_2), 3.58 (s, 1H), 3.20 (s, 3H, SO_2CH_3), 2.80-2.55 (m, 2H), 2.08 (s, 6H), 1.87-1.23 (m, 6H). ^{13}C NMR (100 MHz, DMSO-d_6) δ 163.0, 162.9,

150.7, 149.1, 148.5, 145.4, 143.1, 140.0, 131.8, 131.6, 129.4, 128.4, 127.0, 119.5, 115.2, 96.6, 69.5, 62.6, 52.3, 44.2, 31.8, 16.5. ESI-MS: m/z 546.3 $[M + 1]^+$, 568.2 $[M + Na]^+$. $C_{29}H_{31}N_5O_4S$ (545.21). HPLC purity: 98.33%.

(*E*)-4-(4-((4-(4-(2-cyanovinyl)-2,6-dimethylphenoxy)-5,7-dihydrofuro[3,4-*d*]pyrimidin-2-yl)amino)piperidin-1-yl)benzamide (**13c**)

Yield 47%, white solid, mp 211-212°C. ^{1}H NMR (400 MHz, DMSO-d_6) δ 7.79 (d, *J* = 7.9 Hz, 2H, C_3,C_5-Ph'-H), 7.60 (d, *J* = 16.7 Hz, 1H, ArCH═), 7.44 (s, 2H, C_3,C_5-Ph-H), 7.45-7.41 (m, 2H), 7.37-7.24 (m, 2H), 6.40 (d, *J* = 16.4 Hz, 1H, ═CHCN), 5.91 (s, 1H, NH), 4.92 (s, 2H, O-CH_2), 4.80 (s, 2H, O-CH_2), 3.62 (s, 1H), 2.83-2.72 (m, 2H), 2.08 (s, 6H), 1.90-1.22 (m, 6H). ^{13}C NMR (100 MHz, DMSO-d_6) δ 163.1, 162.7, 150.7, 148.7, 145.1, 143.0, 139.7, 132.0, 129.4, 128.7, 127.1, 119.3, 118.7, 115.8, 104.6, 69.7, 62.1, 52.3, 31.9, 16.5. ESI-MS: m/z 511.3 $[M + 1]^+$, 533.6 $[M + Na]^+$. $C_{29}H_{30}N_6O_3$ (510.24). HPLC purity: 98.94%.

(E)-3-(3,5-dimethyl-4-((2-((1-(4-nitrophenyl)piperidin-4-yl)amino)-5,7-dihydrofuro[3,4-d]pyrimidin-4-yl)oxy)phenyl)acrylonitrile (**13d**)

Yield 55%, white solid, mp 236-238°C. ^{1}H NMR (400 MHz, DMSO-d_6) δ 7.67-7.60 (m, 3H), 7.44 (s, 2H, C_3,C_5-Ph-H), 6.51 (d, *J* = 7.2 Hz, 2H), 6.42 (d, *J* = 16.1 Hz, 1H, ═CHCN), 5.90 (s, 1H, NH), 4.90 (s, 2H, O-CH_2), 4.78 (s, 2H, O-CH_2), 3.60 (s, 1H), 2.74-2.71 (m, 2H), 2.10 (s, 6H), 1.92-1.35 (m, 6H). ESI-MS: m/z 513.2 $[M + 1]^+$, 535.3 $[M + Na]^+$. $C_{28}H_{28}N_6O_4$ (512.22).

(*E*)-3-(4-((2-((1-(4-aminophenyl)piperidin-4-yl)amino)-5,7-dihydrofuro[3,4-*d*]pyrimidin-4-yl)oxy)-3,5-dimethylphenyl)acrylonitrile (**14a**)

Compound **13d** (0.30 g, 1.17 mmol) was added to a solution of 10% Pa/C (0.064 g, 0.03mmol) in MeOH (20 mL). The reaction reacted for overnight in hydrogen. Then the solution was filtered and purified to obtain **14a**. Yield 62%, white solid, mp 148-150°C. ^{1}H NMR (400 MHz, DMSO-d_6) δ 7.67-7.60 (m, 3H), 7.44 (s, 2H, C_3,C_5-Ph-H), 6.51 (d, J = 7.2 Hz, 2H), 6.42 (d, J = 16.7 Hz, 1H, ＝CHCN), 5.92 (s, 1H, NH), 4.92 (s, 2H, O-CH_2), 4.78 (s, 2H, O-CH_2), 4.58 (s, 2H, NH_2), 3.61-3.60 (m, 1H), 2.87-2.70 (m, 2H), 2.08 (s, 6H), 1.90 – 1.04 (m, 6H). ^{13}C NMR (100 MHz, DMSO-d_6) δ 163.1, 162.9, 150.4, 143.1, 142.5, 131.8, 131.6, 128.5, 119.3, 119.0, 115.1, 96.6, 72.4, 69.5, 50.7, 31.8, 16.5. ESI-MS: m/z 483.1 $[M + 1]^+$, 505.3 $[M + Na]^+$. $C_{28}H_{30}N_6O_2$ (482.24). HPLC purity: 97.59%.

(*E*)-N-(4-(4-((4-(4-(2-cyanovinyl)-2,6-dimethylphenoxy)-5,7-dihydrofuro[3,4-*d*]pyrimidin-2-yl)amino)piperidin-1-yl)phenyl)methanesulfonamide (**14b**)

The synthesis procedure is the same as compounds **8a-j**, the difference is that the reactive material is **14a** (0.48g, 1.0 mmol). Yield 64%, white solid, mp 165-167°C. ^{1}H NMR (400 MHz, DMSO-d_6) δ 9.72 (s, 1H, NH), 7.69-7.63 (m, 2H), 7.60-7.58 (m, 1H, ArCH＝), 7.56 (d, J = 7.8 Hz, 2H), 7.44 (s, 2H, C_3,C_5-Ph-H), 6.42 (d, J = 16.7 Hz, 1H, ＝CHCN), 5.90 (s, 1H, NH), 4.92 (m, 2H, O-CH_2), 4.76 (s, 2H, O-CH_2), 3.63-3.54 (m, 1H), 3.21 (s, 3H, SO_2CH_3), 2.85-2.61 (m, 2H), 2.08 (s, 6H), 1.91-1.18 (m, 6H). ^{13}C NMR (100 MHz, DMSO-d_6) δ 163.0, 162.8, 150.7, 149.2, 148.5, 145.4, 143.2, 139.6, 131.6, 129.4, 128.5, 127.0, 119.4, 115.4, 96.6, 69.5, 62.6, 52.6, 44.1, 31.8, 16.5. ESI-MS: m/z 561.4 $[M + 1]^+$, 583.5 $[M + Na]^+$. $C_{29}H_{32}N_6O_4S$ (560.22). HPLC purity: 98.94%.

(*E*)-N-(4-(4-((4-(4-(2-cyanovinyl)-2,6-dimethylphenoxy)-5,7-dihydrofuro[3,4-*d*]pyrimidin-2-yl)amino)piperidin-1-yl)phenyl)aminosulfonamide (**14c**)

The synthesis procedure is the same as compounds **8a-j**, the difference is that the reactive material is **14a** (0.48g, 1.0 mmol). Yield 27%, white solid, mp 181-183°C. ^{1}H NMR (400 MHz, DMSO-d_6) δ 9.69 (s, 1H, NH), 7.67-7.60 (m, 3H), 7.50-7.48 (m, 2H), 7.44 (s, 2H, C_3,C_5-Ph-H), 6.51 (d, J = 7.2 Hz, 2H), 6.42 (d, J = 16.4 Hz, 1H, ═CHCN), 5.91 (s, 1H, NH), 4.93 (s, 2H, O-CH_2), 4.80 (s, 2H, O-CH_2), 3.62 (s, 1H), 2.88-2.68 (m, 2H), 2.08 (s, 6H), 1.97 – 1.14 (m, 6H). ^{13}C NMR (100 MHz, DMSO-d_6) δ 163.0, 162.9, 150.7, 148.5, 143.1, 131.8, 129.4, 128.9, 128.5, 126.9, 119.3, 119.0, 115.7, 96.6, 69.5, 62.0, 52.6, 31.8, 16.5. ESI-MS: m/z 562.3 $[M + 1]^+$. $C_{28}H_{31}N_7O_4S$ (561.22). HPLC purity: 97.00%.

(*E*)-3-(3,5-dimethyl-4-((2-(piperidin-4-ylamino)-5,7-dihydrofuro[3,4-*d*]pyrimidin-4-yl)oxy)phenyl)acrylonitrile (**15**)

A solution of **6** (2.06 g, 6.34 mmol), 4-amino-1-Boc-piperidine (1.52 g, 7.60 mmol), and K_2CO_3 (1.74 g, 12.6 mmol) in DMF (30 mL) was heated at 120°C for 6 h (monitored by TLC). 100 mL water was added when the solution was cooled down to room temperature. The obtained white solid was filtered and dried. Then the dried product was added DCM (5 mL) and TFA (4.44 mL, 60 mmol), and the reaction continued for 5 h at room temperature. Then the mixture was alkalized (pH = 9) with $NaHCO_3$ solution, and extracted with DCM. The combined DCM phase was purified by flash column chromatography obtained intermediate **15** as a white solid, 66% yield, mp 174-176°C. ^{1}H NMR (400 MHz, DMSO-d_6) δ 7.60 (d, J = 16.7 Hz, 1H, ArCH═),

7.44 (s, 2H), 7.01 (s, 1H, NH), 6.40 (d, *J* = 16.1 Hz, 1H, ＝CHCN), 4.90 (s, 2H, O-CH_2), 4.78 (s, 2H, O-CH_2), 3.74-3.71 (m, 1H), 2.85-2.74 (m, 2H), 2.10 (s, 6H), 1.91-1.24 (m, 6H). ESI-MS: m/z 392.4 $[M + 1]^+$. $C_{22}H_{25}N_5O_2$ (391.20).

General Synthesis Procedure for 16a-f

Compounds **15** (0.39 g, 1.0 mmol), K_2CO_3 (0.28 g, 2.0 mmol) and substituted benzyl chloride (bromine) (1.2 mmol) were added in anhydrous DMF (10 mL). The mixture reacted for 3-8 h at room temperature. Then water (100 mL) was added and the mixed solution was extracted with EA. Then the organic phase was purified and recrystallized from EA/PE afforded the final compounds **16a−f**.

(*E*)-4-((4-((4-(4-(2-cyanovinyl)-2,6-dimethylphenoxy)-5,7-dihydrofuro[3,4-*d*]pyrimidin-2-yl)amino)piperidin-1-yl)methyl)benzenesulfonamide (**16a**)

Yield 84%, white solid, mp 208-210°C. ^{1}H NMR (400 MHz, DMSO-d_6) δ 7.78 (d, *J* = 7.8 Hz, 2H), 7.60 (d, *J* = 16.4 Hz, 1H, ArCH＝), 7.48-7.45 (m, 4H), 7.37-7.24 (m, 2H), 7.08 (s, 1H, NH), 6.41 (d, *J* = 16.7 Hz, 1H, ＝CHCN), 4.92 (s, 2H, O-CH_2), 4.76 (s, 2H, O-CH_2), 3.78-3.37 (m, 3H), 2.92-2.56 (m, 2H), 2.08 (s, 6H), 1.88-1.13 (m, 6H). ^{13}C NMR (100 MHz, DMSO-d_6) δ 163.0, 162.9, 150.5, 148.5, 143.1, 131.7, 131.6, 129.4, 128.9, 128.3, 126.9, 126.0, 119.3, 96.6, 69.4, 61.9, 52.6, 31.6, 16.5. ESI-MS: m/z 561.3 $[M + 1]^+$, 583.4 $[M + Na]^+$. $C_{29}H_{32}N_6O_4S$ (560.22). HPLC purity: 98.17%.

(*E*)-3-(3,5-dimethyl-4-((2-((1-(4-(methylsulfonyl)benzyl)piperidin-4-yl)amino)-5,7-dihydrofuro[3,4-*d*]pyrimidin-4-yl)oxy)phenyl)acrylonitrile (**16b**)

Yield 82%, white solid, mp 215-217°C. ^{1}H NMR (400 MHz, DMSO-d_6) δ

7.90-7.86 (m, 2H), 7.60-7.58 (m, 1H, ArCH═), 7.54 (d, *J* = 7.8 Hz, 2H), 7.44 (s, 2H, C_3,C_5-Ph-H), 7.31-6.99 (m, 1H), 6.40 (d, *J* = 16.6 Hz, 1H, ═CHCN), 5.00-4.87 (m, 2H, O-CH_2), 4.76 (s, 2H, O-CH_2), 3.63-3.39 (m, 3H), 3.20 (s, 3H, SO_2CH_3), 2.85-2.56 (m, 2H), 2.08 (s, 6H), 1.83-1.07 (m, 6H). ^{13}C NMR (100 MHz, DMSO-d_6) δ 163.0, 162.9, 150.5, 149.2, 148.5, 145.4, 139.8, 139.5, 131.7, 131.6, 129.7, 128.5, 127.3, 119.4, 96.6, 72.4, 69.5, 62.6, 61.8, 52.6, 44.1, 31.6, 16.5. ESI-MS: m/z 560.2 $[M + 1]^+$, 582.8 $[M + Na]^+$. $C_{30}H_{33}N_5O_4S$ (559.23). HPLC purity: 98.05%.

(*E*)-4-((4-((4-(4-(2-cyanovinyl)-2,6-dimethylphenoxy)-5,7-dihydrofuro[3,4-*d*]pyrimidin-2-yl)amino)piperidin-1-yl)methyl)benzamide (**16c**)

Yield 74%, white solid, mp 188-190°C. ^{1}H NMR (400 MHz, DMSO-d_6) δ 7.79 (d, *J* = 8.0 Hz, 2H), 7.60 (d, *J* = 16.3 Hz, 1H, ArCH═), 7.54-7.45 (m, 2H), 7.44 (m, 2H, C_3,C_5-Ph-H), 7.37-7.24 (m, 2H), 7.07 (s, 1H, NH), 6.40 (d, *J* = 16.4 Hz, 1H, ═CHCN), 4.94-4.92 (m, 2H, O-CH_2), 4.76 (s, 2H, O-CH_2), 3.65-3.37 (m, 3H), 2.90-2.61 (m, 2H), 2.08 (s, 6H), 1.88-1.09 (m, 6H). ^{13}C NMR (100 MHz, DMSO-d_6) δ 163.0, 162.8, 150.5, 148.5, 143.1, 139.5, 131.8, 129.4, 128.9, 128.5, 127.0, 126.3, 119.3, 96.6, 72.5, 69.4, 61.7, 52.6, 31.6, 16.5. ESI-MS: m/z 525.3 $[M + 1]^+$, 547.5 $[M + Na]^+$. $C_{30}H_{32}N_6O_3$ (524.25). HPLC purity: 97.28%.

(*E*)-3-(3,5-dimethyl-4-((2-((1-(4-nitrobenzyl)piperidin-4-yl)amino)-5,7-dihydrofuro[3,4-*d*]pyrimidin-4-yl)oxy)phenyl)acrylonitrile (**16d**)

Yield 88%, white solid, mp 184-186°C. ^{1}H NMR (400 MHz, DMSO-d_6) δ 8.19 (d, *J* = 8.3 Hz, 2H, C_3,C_5-Ph'-H), 7.61-7.54 (m, 3H), 7.44 (s, 2H, C_3,C_5-Ph-H), 7.36-7.00 (m, 1H), 6.40 (d, *J* = 16.6 Hz, 1H, ═CHCN), 4.90 (s, 2H, O-CH_2), 4.76 (s,

2H, O-CH_2), 3.64-3.44 (m, 3H), 2.87-2.58 (m, 2H), 2.07 (s, 6H), 1.87-1.16 (m, 6H). ^{13}C NMR (100 MHz, DMSO-d_6) δ 163.1, 162.9, 150.5, 148.5, 147.5, 146.9, 131.7, 131.6, 130.0, 128.5, 123.8, 119.3, 96.6, 72.3, 69.5, 61.6, 52.6, 31.6, 29.0, 26.8, 16.5. ESI-MS: m/z 527.5 $[M + 1]^+$. $C_{29}H_{30}N_6O_4$ (526.23). HPLC purity: 96.76%.

(*E*)-3-(4-((2-((1-(4-aminobenzyl)piperidin-4-yl)amino)-5,7-dihydrofuro[3,4-*d*]pyrimidin-4-yl)oxy)-3,5-dimethylphenyl)acrylonitrile (**16e**)

Yield 51%, white solid, mp 173-175°C. ^{1}H NMR (400 MHz, DMSO-d_6) δ 7.66-7.55 (m, 2H), 7.45 (s, 2H, C_3,C_5-Ph-H), 7.08-7.05 (m, 1H), 6.54 (d, J = 7.0 Hz, 2H), 6.42 (d, J = 16.7 Hz, 1H, ＝CHCN), 5.89 (s, 1H, NH), 5.28 (s, 2H, NH_2), 4.92 (s, 2H, O-CH_2), 4.77 (s, 2H, O-CH_2), 4.09-3.60 (m, 3H), 2.87-2.70 (m, 2H), 2.08 (s, 6H), 1.90-1.04 (m, 6H). ^{13}C NMR (100 MHz, DMSO-d_6) δ 163.0, 162.7, 150.4, 148.5, 131.7, 128.5, 123.7, 119.3, 118.3, 113.9, 96.7, 95.6, 72.4, 69.5, 29.5, 16.6. ESI-MS: m/z 497.5 $[M + 1]^+$, 519.7 $[M + Na]^+$. $C_{29}H_{32}N_6O_2$ (496.26). HPLC purity: 96.58%.

(*E*)-3-(3,5-dimethyl-4-((2-((1-(4-(trifluoromethyl)benzyl)piperidin-4-yl)amino)-5,7-dihydrofuro[3,4-*d*]pyrimidin-4-yl)oxy)phenyl)acrylonitrile (**16f**)

Yield 77%, white solid, mp 231-233°C. ^{1}H NMR (400 MHz, DMSO-d_6) δ 7.67 (d, J = 7.8 Hz, 2H, C_3,C_5-Ph'-H), 7.64-7.55 (m, 1H), 7.49 (d, J = 7.9 Hz, 2H, C_2,C_6-Ph'-H), 7.44 (s, 2H, C_3,C_5-Ph-H), 7.24-7.08 (m, 1H), 6.40 (d, J = 16.7 Hz, 1H, ＝CHCN), 4.90 (s, 2H, O-CH_2), 4.76 (s, 2H, O-CH_2), 3.57-3.39 (m, 2H), 2.82-2.56 (m, 3H), 2.07 (s, 6H), 1.93-1.13 (m, 6H). ^{13}C NMR (100 MHz, DMSO-d_6) δ 163.0, 162.9, 150.5, 144.2, 131.7, 131.6, 129.7, 128.5, 126.1, 125.5, 125.4, 123.4, 119.3, 96.7, 69.4, 61.9, 52.6, 31.5, 29.0, 16.5. ESI-MS: m/z 550.2 $[M + 1]^+$. $C_{30}H_{30}F_3N_5O_2$

(549.24). HPLC purity: 97.11%.

(*E*)-3-(3,5-dimethyl-4-((2-((4-(piperazin-1-ylmethyl)phenyl)amino)-5,7-dihydrofuro[3,4-d]pyrimidin-4-yl)oxy)phenyl)acrylonitrile (**17**)

The synthesis procedure is the same as compound **7**, the difference is that the reactive material is *tert*-butyl 4-(4-aminobenzyl)piperazine-1-carboxylate (1.2 mmol). Yield 42%, white solid, mp 177-179°C. ^{1}H NMR (400 MHz, DMSO-d_6) δ 9.61 (s, 1H, NH), 7.68 (d, J = 16.4 Hz, 1H, ArCH═), 7.44 (s, 2H, C_3,C_5-Ph-H), 7.23 (d, J = 7.9 Hz, 2H, C_3,C_5-Ph'-H), 6.91-6.89 (m, 2H), 6.51 (d, J = 16.1 Hz, 1H, ═CHCN), 4.90 (s, 2H, O-CH_2), 4.76 (s, 2H, O-CH_2), 3.37 (s, 2H, Ph-CH_2), 3.09 (t, J = 4.8 Hz, 4H), 2.39-2.36 (m, 4H), 2.10 (s, 6H). ESI-MS: m/z 483.1 $[M + 1]^+$, 505.4 $[M + Na]^+$. $C_{28}H_{30}N_6O2$ (482.24).

(*E*)-4-(4-((4-(4-(2-cyanovinyl)-2,6-dimethylphenoxy)-5,7-dihydrofuro[3,4-*d*]pyrimidin-2-yl)amino)benzyl)piperazine-1-sulfonamide (**18a**)

The synthesis procedure is the same as compounds **8a-j**, the difference is that the reactive material is compound **17** (0.48 g, 1.0 mmol). Yield 29%, white solid, mp 185-187°C. ^{1}H NMR (400 MHz, DMSO-d_6) δ 9.67 (s, 1H, NH), 7.68 (d, J = 16.4 Hz, 1H, ArCH═), 7.52 (s, 2H, C_3,C_5-Ph-H), 7.48-7.45 (m, 2H), 7.25 (d, J = 8.1 Hz, 2H, C_3,C_5-Ph'-H), 6.90 (d, J = 8.1 Hz, 2H, C_2,C_6-Ph'-H), 6.51 (d, J = 16.7 Hz, 1H, ═CHCN), 5.04 (s, 2H, O-CH_2), 4.90 (s, 2H, O-CH_2), 3.39 (s, 2H, Ph-CH_2), 3.09 (t, J = 4.8 Hz, 4H, C_3,C_5-piperazine-H), 2.39 (t, J = 4.8 Hz, 4H, C_2,C_6-piperazine-H), 2.10 (s, 6H). ^{13}C NMR (100 MHz, DMSO-d_6) δ 173.9, 162.8, 160.6, 152.2, 150.5, 139.5, 131.9, 131.8, 130.8, 129.1, 128.6, 119.4, 118.6, 104.5, 96.8, 72.2, 69.5, 61.5, 52.1,

45.9, 16.5. ESI-MS: m/z 562.2 $[M + 1]^+$, 584.5 $[M + Na]^+$. $C_{28}H_{31}N_7O_4S$ (561.22). HPLC purity: 96.58%.

(*E*)-3-(3,5-dimethyl-4-((2-((4-((4-(methylsulfonyl)piperazin-1-yl)methyl)phenyl)amino)-5,7-dihydrofuro[3,4-*d*]pyrimidin-4-yl)oxy)phenyl)acrylonitrile (**18b**)

The synthesis procedure is the same as compounds **8a-j**, the difference is that the reactive material is compound **17** (0.48 g, 1.0 mmol). Yield 79%, white solid, mp 211-213°C. ^{1}H NMR (400 MHz, DMSO-d_6) δ 9.69 (s, 1H, NH), 7.69 (d, J = 16.7 Hz, 1H, ArCH═), 7.54 (s, 2H, C_3,C_5-Ph-H), 7.25 (d, J = 7.7 Hz, 2H, C_3,C_5-Ph'-H), 6.91 (d, J = 8.1 Hz, 2H, C_2,C_6-Ph'-H), 6.50 (d, J = 16.7 Hz, 1H, ═CHCN), 5.06 (s, 2H, O-CH_2), 4.88 (s, 2H, O-CH_2), 3.37 (s, 2H, Ph-CH_2), 3.09 (t, J = 4.9 Hz, 4H, C_3,C_5-piperazine-H), 2.88 (s, 3H, SO_2CH_3), 2.39 (t, J = 4.8 Hz, 4H, C_2,C_6-piperazine-H), 2.10 (s, 6H). ^{13}C NMR (100 MHz, DMSO-d_6) δ 173.9, 162.8, 160.6, 152.2, 150.5, 139.5, 131.9, 131.8, 130.8, 129.1, 128.6, 119.4, 118.6, 104.5, 96.8, 72.2, 69.5, 61.5, 52.1, 45.9, 34.1, 16.5. ESI-MS: m/z 561.4 $[M + 1]^+$, 583.6 $[M + Na]^+$. $C_{29}H_{32}N_6O_4S$ (560.22). HPLC purity: 99.22%.

ASSOCIATED CONTENT

Supporting Information includes:

The synthetic procedure of compounds **8c-j**, *in vitro* assay of anti-HIV activities, HIV-1 reverse transcriptase (RT) inhibitory assays, pharmacokinetic and acute toxicity experiment methods.

AUTHOR INFORMATION

Corresponding Authors

*D.K.: e-mail, kangdongwei@sdu.edu.cn; tel, 086-531-88382005;

*P.Z.: e-mail, zhanpeng1982@sdu.edu.cn; tel, 086-531-88382005;

*X.L.: e-mail, xinyongl@sdu.edu.cn; tel, 086-531-88380270.

Notes

The authors declare that all experimental work complied with the institutional guidelines on animal studies (care and use of laboratory animals).

The authors declare no competing financial interest.

ACKNOWLEDGMENTS

We gratefully acknowledge financial support from the National Natural Science Foundation of China (NSFC 81903453, 81973181), Shandong Provincial Natural Science Foundation (ZR2020YQ61, ZR2020JQ31, ZR2019BH011), Foreign Cultural and Educational Experts Project (GXL20200015001), Shandong Provincial Key Research and Development Project (Nos. 2019JZZY021011), Qilu Young Scholars Program of Shandong University and Taishan Scholar Program of Shandong Province.

ABBREVIATIONS USED

AIDS, acquired immune deficiency syndrome; DLV, delavirdine; DOR, Doravirine; EFV, efavirenz; ETR, etravirine; FDA, U.S. Food and Drug Administration; HAART, highly active antiretroviral therapy; HIV, human immunodeficiency virus; NNIBP, NNRTIs-binding pocket; NNRTIs, non-nucleoside RT inhibitors; NVP, nevirapine; RPV, rilpivirine; RT, reverse transcriptase; SARs, structure-activity relationships; SI, selectivity index; TLC, thin layer chromatography; WT, wild type.

REFERENCES

1. Fauci, A. S.; Lane, H. C. Four decades of HIV/AIDS - much accomplished, much to do. *N. Engl. J. Med.* **2020,** *383*, 1-4.
2. Battini, L.; Bollini, M. Challenges and approaches in the discovery of human immunodeficiency virus type-1 non-nucleoside reverse transcriptase inhibitors. *Med. Res. Rev.* **2019,** *39*, 1235-1273.
3. Zhan, P.; Pannecouque, C.; De Clercq, E.; Liu, X. Anti-HIV drug discovery and development: current innovations and future trends. *J. Med. Chem.* **2016,** *59*, 2849-2878.
4. Bec, G.; Meyer, B.; Gerard, M.-A.; Steger, J.; Fauster, K.; Wolff, P.; Burnouf, D.; Micura, R.; Dumas, P.; Ennifar, E. Thermodynamics of HIV-1 reverse transcriptase in action elucidates the mechanism of action of non-nucleoside inhibitors. *J. Am. Chem. Soc.* **2013,** *135*, 9743-9752.
5. Namasivayam, V.; Vanangamudi, M.; Kramer, V. G.; Kurup, S.; Zhan, P.; Liu, X.; Kongsted, J.; Byrareddy, S. N. The journey of HIV-1 non-nucleoside reverse transcriptase inhibitors (NNRTIs) from lab to clinic. *J. Med. Chem.* **2019,** *62*, 4851-4883.
6. Lehman, D. A.; Wamalwa, D. C.; McCoy, C. O.; Matsen, F. A.; Langat, A.; Chohan, B. H.; Benki-Nugent, S.; Custers-Allen, R.; Bushman, F. D.; John-Stewart, G. C.; Overbaugh, J. Low-frequency nevirapine resistance at multiple sites may predict treatment failure in infants on nevirapine-based treatment. *J. Acquired Immune Defic.Syndr.* **2012,** *60*, 225-233.
7. Cilento, M. E.; Kirby, K. A.; Sarafianos, S. G. Avoiding drug resistance in HIV reverse transcriptase. *Chem. Rev.* **2021,** *121*, 3271-3296.
8. Beyrer, C.; Pozniak, A. HIV drug resistance - an emerging threat to epidemic control. *N. Engl. J. Med.* **2017,** *377*, 1605-1607.
9. Kang, D.; Ruiz, F. X.; Sun, Y.; Feng, D.; Jing, L.; Wang, Z.; Zhang, T.; Gao, S.; Sun, L.; De Clercq, E.; Pannecouque, C.; Arnold, E.; Zhan, P.; Liu, X. 2,4,5-trisubstituted pyrimidines as potent HIV-1 NNRTIs: rational design, synthesis, activity evaluation, and crystallographic studies. *J. Med. Chem.* **2021,** *64*, 4239-4256.
10. Kang, D.; Zhang, H.; Wang, Z.; Zhao, T.; Ginex, T.; Luque, F. J.; Yang, Y.; Wu, G.; Feng, D.; Wei, F.; Zhang, J.; De Clercq, E.; Pannecouque, C.; Chen, C. H.; Lee, K.-H.; Murugan, N. A.; Steitz, T. A.; Zhan, P.; Liu, X. Identification of dihydrofuro 3,4-d pyrimidine derivatives as novel HIV-1 non-nucleoside reverse transcriptase inhibitors with promising antiviral activities and desirable physicochemical properties. *J. Med. Chem.* **2019,** *62*, 1484-1501.
11. Kang, D.; Fang, Z.; Li, Z.; Huang, B.; Zhang, H.; Lu, X.; Xu, H.; Zhou, Z.; Ding, X.; Daelemans, D.; De Clercq, E.; Pannecouque, C.; Zhan, P.; Liu, X. Design, synthesis, and evaluation of thiophene [3,2-*d*]pyrimidine derivatives as HIV-1 non-nucleoside reverse transcriptase inhibitors with significantly improved drug resistance profiles. *J. Med. Chem.* **2016,** *59*, 7991-8007.
12. Kang, D.; Fang, Z.; Huang, B.; Lu, X.; Zhang, H.; Xu, H.; Huo, Z.; Zhou, Z.; Yu, Z.; Meng, Q.; Wu, G.; Ding, X.; Tian, Y.; Daelemans, D.; De Clercq, E.; Pannecouque, C.; Zhan, P.; Liu, X. Structure-based optimization of thiophene[3,2-*d*]pyrimidine derivatives as potent HIV-1 non-nucleoside reverse transcriptase inhibitors with improved potency against resistance-associated variants. *J. Med. Chem.* **2017,** *60*, 4424-4443.
13. Kang, D.; Ruiz, F. X.; Feng, D.; Pilch, A.; Zhao, T.; Wei, F.; Wang, Z.; Sun, Y.; Fang, Z.; De Clercq, E.; Pannecouque, C.; Arnold, E.; Liu, X.; Zhan, P. Discovery and characterization of fluorine-substituted diarylpyrimidine derivatives as novel HIV-1 NNRTIs with highly improved resistance profiles and low activity for the hERG ion channel. *J. Med. Chem.* **2020,** *63*, 1298-1312.

14. Kang, D.; Feng, D.; Ginex, T.; Zou, J.; Wei, F.; Zhao, T.; Huang, B.; Sun, Y.; Desta, S.; De Clercq, E.; Pannecouque, C.; Zhan, P.; Liu, X. Exploring the hydrophobic channel of NNIBP leads to the discovery of novel piperidine-substituted thiophene[3,2-*d*]pyrimidine derivatives as potent HIV-1 NNRTIs. *Acta Pharm. Sin. B* **2020,** *10*, 878-894.
15. Zhuang, C.; Pannecouque, C.; De Clercq, E.; Chen, F. Development of non-nucleoside reverse transcriptase inhibitors (NNRTIs): our past twenty years. *Acta Pharm. Sin. B* **2020,** *10*, 961-978.
16. Ding, L.; Zhuang, C.; Chen, F. Druggability modification strategies of the diarylpyrimidine-type non-nucleoside reverse transcriptase inhibitors. *Med. Res. Rev.* **2021,** *41*, 1255-1290.
17. Wang, Z.; Zalloum, W. A.; Wang, W.; Jiang, X.; De Clercq, E.; Pannecouque, C.; Kang, D.; Zhan, P.; Liu, X. Discovery of novel dihydrothiopyrano[4,3-*d*]pyrimidine derivatives as potent HIV-1 NNRTIs with significantly reduced hERG inhibitory activity and improved resistance profiles. *J. Med. Chem.* **2021,** *64*, 13658-13675.
18. Pannecouque, C.; Daelemans, D.; De Clercq, E. Tetrazolium-based colorimetric assay for the detection of HIV replication inhibitors: revisited 20 years later. *Nat. Protoc.* **2008,** *3*, 427-434.
19. Wang, Z.; Yu, Z.; Kang, D.; Zhang, J.; Tian, Y.; Daelemans, D.; De Clercq, E.; Pannecouque, C.; Zhan, P.; Liu, X. Design, synthesis and biological evaluation of novel acetamide-substituted doravirine and its prodrugs as potent HIV-1 NNRTIs. *Bioorg. Med. Chem.* **2019**, *27*, 447-456.
20. Suzuki, K.; Craddock, B. P.; Okamoto, N.; Kano, T.; Steigbigel, R. T. Poly A-linked colorimetric microtiter plate assay for HIV reverse transcriptase. *J. Virol. Methods* **1993,** *44*, 189-198.
21. Yang, Y.; Kang, D.; Nguyen, L. A.; Smithline, Z. B.; Pannecouque, C.; Zhan, P.; Liu, X.; Steitz, T. A. Structural basis for potent and broad inhibition of HIV-1 RT by thiophene[3,2-*d*]pyrimidine non-nucleoside inhibitors. *eLife* **2018,** *7*, No. e36340.
22. Huang, B.; Chen, W.; Zhao, T.; Li, Z.; Jiang, X.; Ginex, T.; Vílchez, D.; Luque, F. J.; Kang, D.; Gao, P.; Zhang, J.; Tian, Y.; Daelemans, D.; De Clercq, E.; Pannecouque, C.; Zhan, P.; Liu, X. Exploiting the tolerant region I of the non-nucleoside reverse transcriptase inhibitor (NNRTI) binding pocket: discovery of potent diarylpyrimidine-typed HIV-1 NNRTIs against wild-type and E138K mutant virus with significantly improved water solubility and favorable safety profiles. *J. Med. Chem.* **2019,** *62*, 2083-2098.

Graphic for manuscript

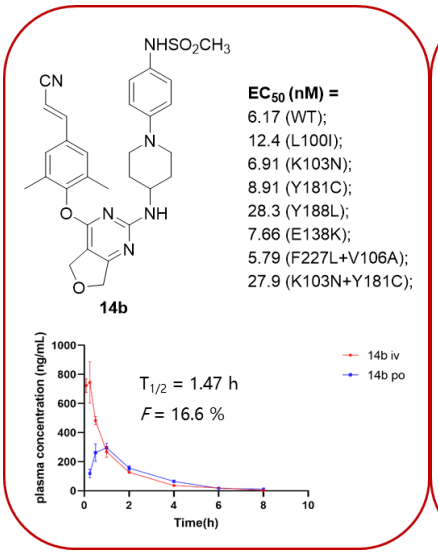

14b

EC_{50} (nM) =
6.17 (WT);
12.4 (L100I);
6.91 (K103N);
8.91 (Y181C);
28.3 (Y188L);
7.66 (E138K);
5.79 (F227L+V106A);
27.9 (K103N+Y181C);

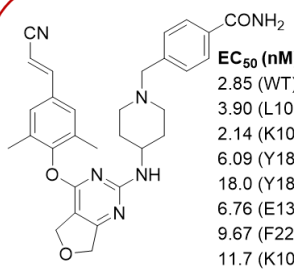

16c

EC_{50} (nM) =
2.85 (WT);
3.90 (L100I);
2.14 (K103N);
6.09 (Y181C);
18.0 (Y188L);
6.76 (E138K);
9.67 (F227L+V106A);
11.7 (K103N+Y181C);